Journal of South American Earth Sciences 105 (2021) 102979

Contents lists available at ScienceDirect

Journal of South American Earth Sciences

journal homepage: www.elsevier.com/locate/jsames

An accumulation of dinosaur remains in fluvial deposits of Mulichinco Formation (lower Valanginian, Neuquén Basin), Patagonia, Argentina: Taphonomic and paleoenvironmental inferences

Diego A. Pino [a,b,c,*], Rodolfo A. Coria [a,b,c], Ignacio Díaz-Martínez [a,b], Maisa A. Tunik [a,b]

[a] Universidad Nacional de Río Negro, Instituto de Investigación en Paleobiología y Geología, Av. Roca 1242, R8332EXZ, General Roca, Río Negro, Argentina
[b] IIPG, UNRN, CONICET, General Roca, Argentina
[c] Consejo Nacional de Investigaciones Científicas y Técnicas (CONICET), Subsecretaria de Cultura de Neuquén - Museo Carmen Funes, Av. Córdoba 55 (8318), Plaza Huincul, Neuquén, Argentina

ARTICLE INFO

Keywords:
Early cretaceous
Fossil vertebrates
Biostratinomic process
Taphonomic alteration mechanism

ABSTRACT

Although the Neuquén Basin (Argentina) has an extensive record of fossil vertebrates for the Upper Cretaceous, little is known about the Early Cretaceous vertebrate faunas. The Mulichinco Formation (early Valanginian), where some dinosaur bone sites were found, provides important additional insights into the composition of continental fauna of that age. Although osteological studies of sauropod and theropod dinosaurs have been published for this unit, no taphonomic studies have been reported to date. Here, we describe the biostratinomic processes that took place on an accumulation of bones found in rocks of the Mulichinco Formation and discuss the relationships between those remains and the environment in which the bones were buried. Taphonomic alteration mechanisms were estimated, including articulation, weathering, abrasion, integrity, bioerosion, transport, and orientation. We described thoroughly a sedimentological section and micro-sections that indicate the stratigraphic location and spatial arrangement of the remains. Three sub-environments in the inferred braided fluvial system were determined and three levels with bones showing different taphonomic attributes were identified within the accumulation. The lag deposits contain indeterminate bone remains with signs of significant transport and probably from different origins. On the other hand, the channel infill contains an articulated carcass of a sauropod and associated remains, of para-autochthonous origin, with no significant transport.

1. Introduction

The Neuquén Basin has one of the most complete vertebrate fossil records in the world (see Leanza et al., 2004 and references therein). Most of this record can be found in units of the Upper Cretaceous Neuquén Group. Yet, recent findings of Lower Cretaceous terrestrial vertebrates on rocks of the Mendoza Group have provided novel data. Generally, the studies performed on both the Neuquén and Mendoza groups were based on systematics and phylogeny of the different taxa involved (Bonaparte, 1991; Coria and Salgado, 1995; Novas, 1996; Salgado et al., 1997; Calvo and González Riga, 2003; Calvo et al., 2004; Coria et al., 2006; among others). Nevertheless, taphonomic studies are very scarce and have been carried out on Late Cretaceous sites (e.g., Previtera, 2011, 2017, 2019).

Regarding the Mendoza Group record, Coria et al. (2010, 2012, 2013) described several sites with continental vertebrate fossils in the Valanginian Mulichinco Formation. There, the holotype specimens of the dicraeosaurid *Pilmatueia faundezi* (Coria et al., 2019) and the carcharodontosaurid *Lajasvenator ascheriae* (Coria et al., 2020) were collected.

In the last years, new accumulations of dinosaur bones from the Mulichinco Formation were excavated closer to the Pilmatué Creek, located 9 km northeast from Las Lajas city (Fig. 1). The main objectives of this contribution are to analyze the taphonomic modification processes present in this bone accumulation, to discuss whether the accumulation was generated in one or more events, and to examine the relationships between the taphonomic history and the paleoenvironment.

* Corresponding author. Universidad Nacional de Río Negro, Instituto de Investigación en Paleobiología y Geología, Av. Roca 1242, R8332EXZ, General Roca, Río Negro, Argentina.
E-mail addresses: dapino@unrn.edu.ar (D.A. Pino), rcoria@unrn.edu.ar (R.A. Coria), idiaz@unrn.edu.ar (I. Díaz-Martínez), mtunik@unrn.edu.ar (M.A. Tunik).

https://doi.org/10.1016/j.jsames.2020.102979
Received 12 August 2020; Received in revised form 19 October 2020; Accepted 19 October 2020
Available online 21 October 2020

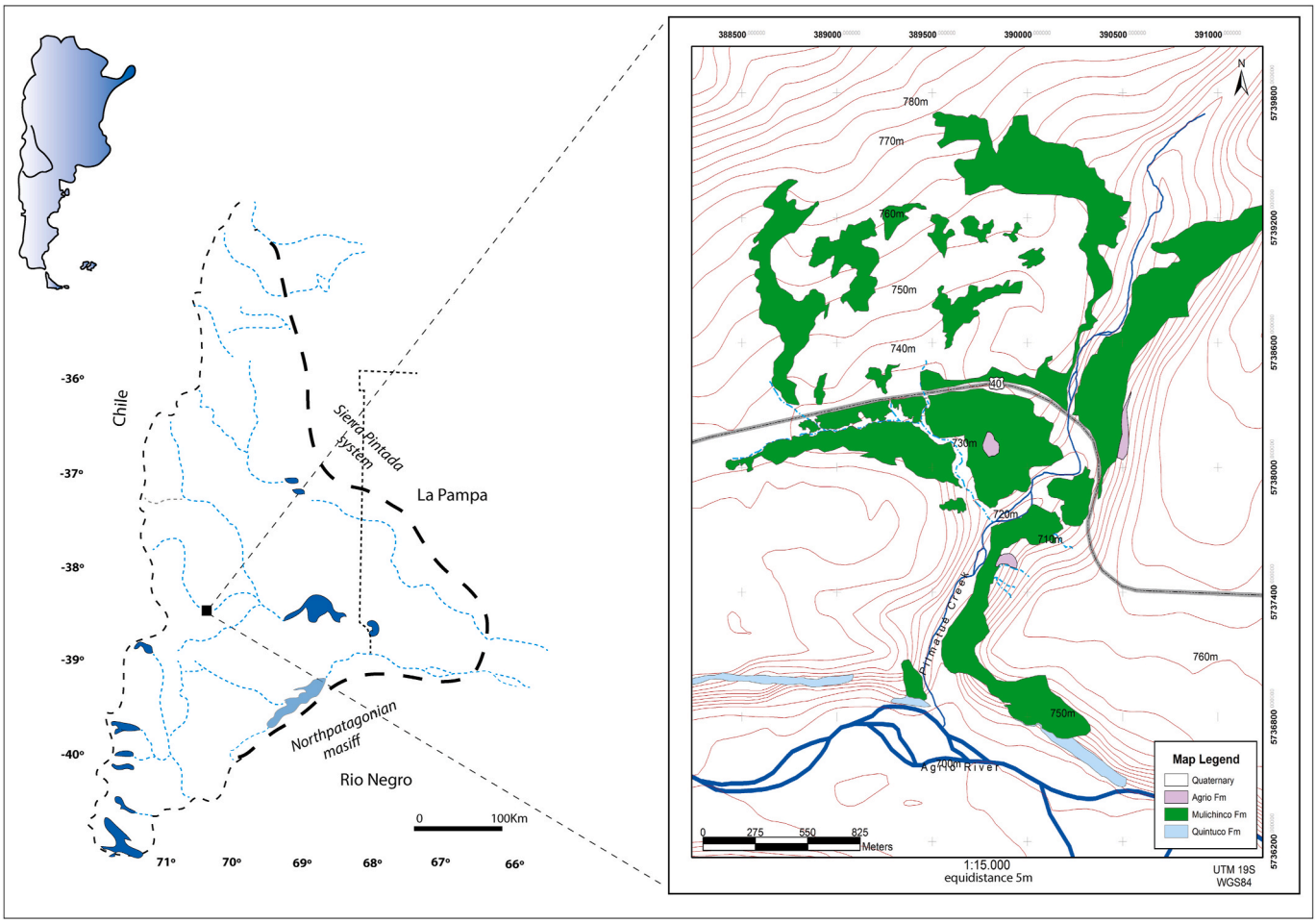

Fig. 1. Location map of the Neuquén Basin showing the outcrops of the Mulichinco Formation in the study area.

2. Geologic setting

The Neuquén basin has three evolutionary stages that span from the Late Triassic to the Late Cenozoic, allowing us to understand its current configuration. From the halfgrabens formed in its initial stage (see D'Elia et al., 2020), followed by the first indicators of subduction and active magmatic arc (Mpodozis and Ramos, 2008; Rossel and Carvajal, 2020), and concluding with variations in the angle of the subducted slab (Ramos, 1999; Ramos and Folguera, 2009), the complexity of the basin can be summed up in three stages or main phases: sinrift, post-rift, and foreland, respectively (see Kietzmann and Folguera, 2020 and references therein).

The Mulichinco Formation (Weaver, 1931), crops out in the center-western sector of the Neuquén Basin, from the north of the Agrio River in the Neuquén province to the south of the province of Mendoza. It is part of the Mendoza Group (Stipanicic et al., 1968), ranging from Kimmeridgian to Barremian (Fig. 2). This unit represents the relative sea-level fall, attributed to tectonic and topographic controls (Schwarz et al., 2006) suffered by the basin after the maximum flooding registered with the deposits of Vaca Muerta and Quintuco formations. This abrupt change from marine and deltaic transitional deposits to conspicuous fluvial deposits is marked by a regional discordance named Intravalanginian by Gulisano et al. (1984) and renamed as Huncálica by Leanza (2009). The Mulichinco Formation is covered by the marine deposits of the Agrio Formation.

Schwarz (2003) made a detailed description of the facies associations and defined the regional and temporal distribution of the deposition systems of this unit. Thus, three regions were established: austral, central, and northern, showing distinctive characteristics in the outcrops at the central-western of the province of Neuquén (Fig. 3). The southern region extends from the Agrio River, 38° 30′S, to latitude 37° 50′S north of the city of Huncal, with a variable thickness of 180–240 m; it is characterized by continental to marginal-marine deposits. The central region extends from the north of the city of Huncal (37° 50′S) to the south of Chos Malal city (37° 30′S), with an approximate thickness of 350 m of deltaic and continental deposits of siliciclastics in the lower section and of sandstones, shales, and limestones of open marine environment in the upper section. Finally, the northern section develops from the south of Chos Malal city (37° 30′S) to the north of the Buta Ranquil area (37 °S); in this sector, the unit is composed of marine siliciclastics and calcareous deposits (see Schwarz, 2003). The studied area is located in the Austral region of the Mulichinco Formation and shows a fining-upward arrangement and a marked decrease in grain size at the cuspidal levels of the section, where remains of marine invertebrates are recognized and attributed to the Agrio Formation. The Mulichinco Formation has an abundant ammonite fauna, indicating an early

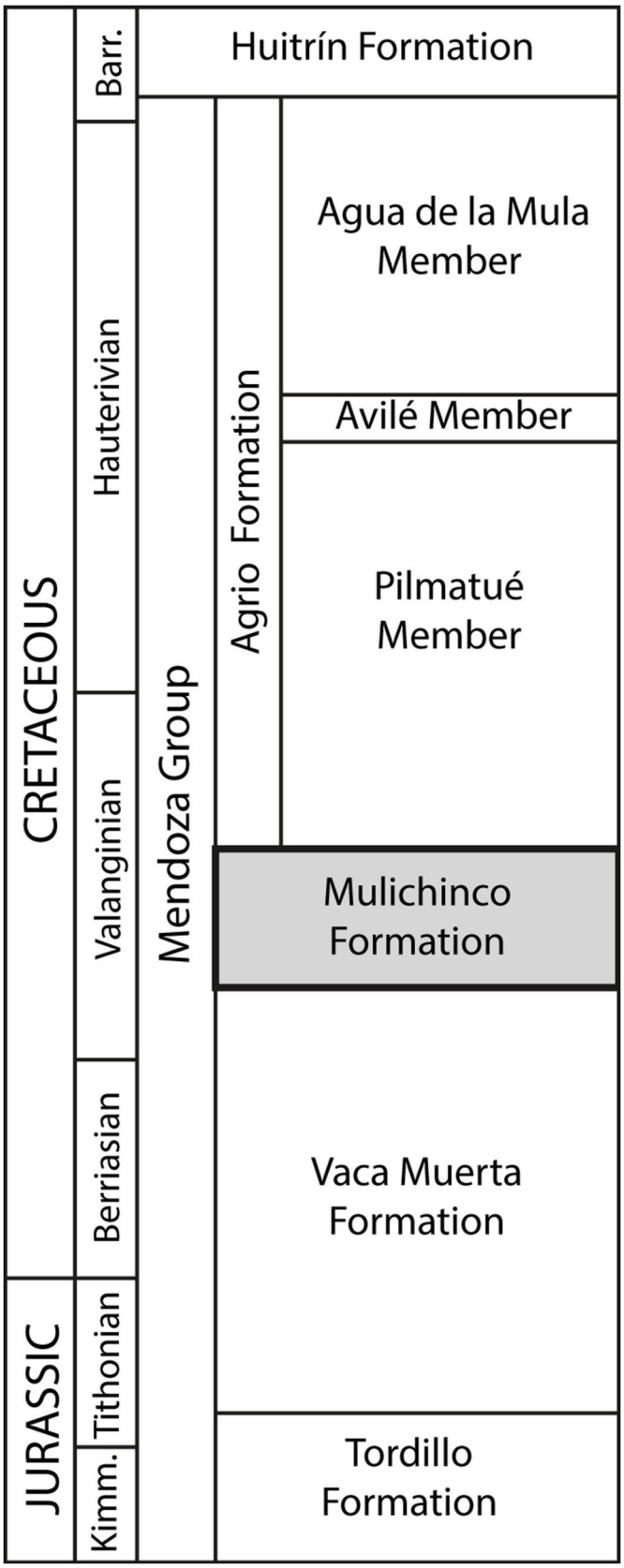

Fig. 2. Simplified stratigraphic scheme of Mendoza Group (modified from Aguirre-Urreta et al., 2017).

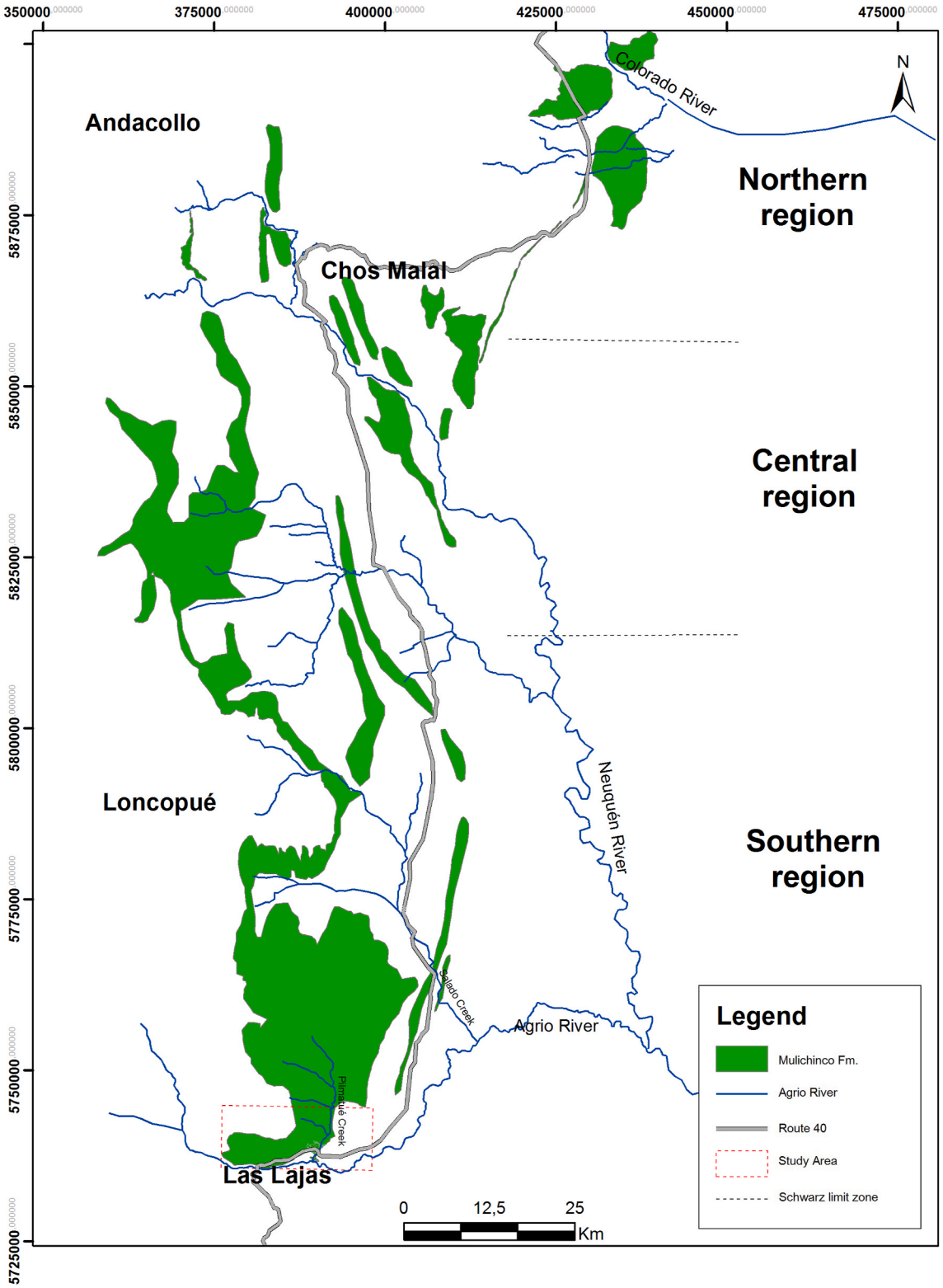

Fig. 3. Map with outcrops of the Mulichinco Formation and the areas established by Schwarz (2003) for the unit (modified from Schwarz et al., 2011).

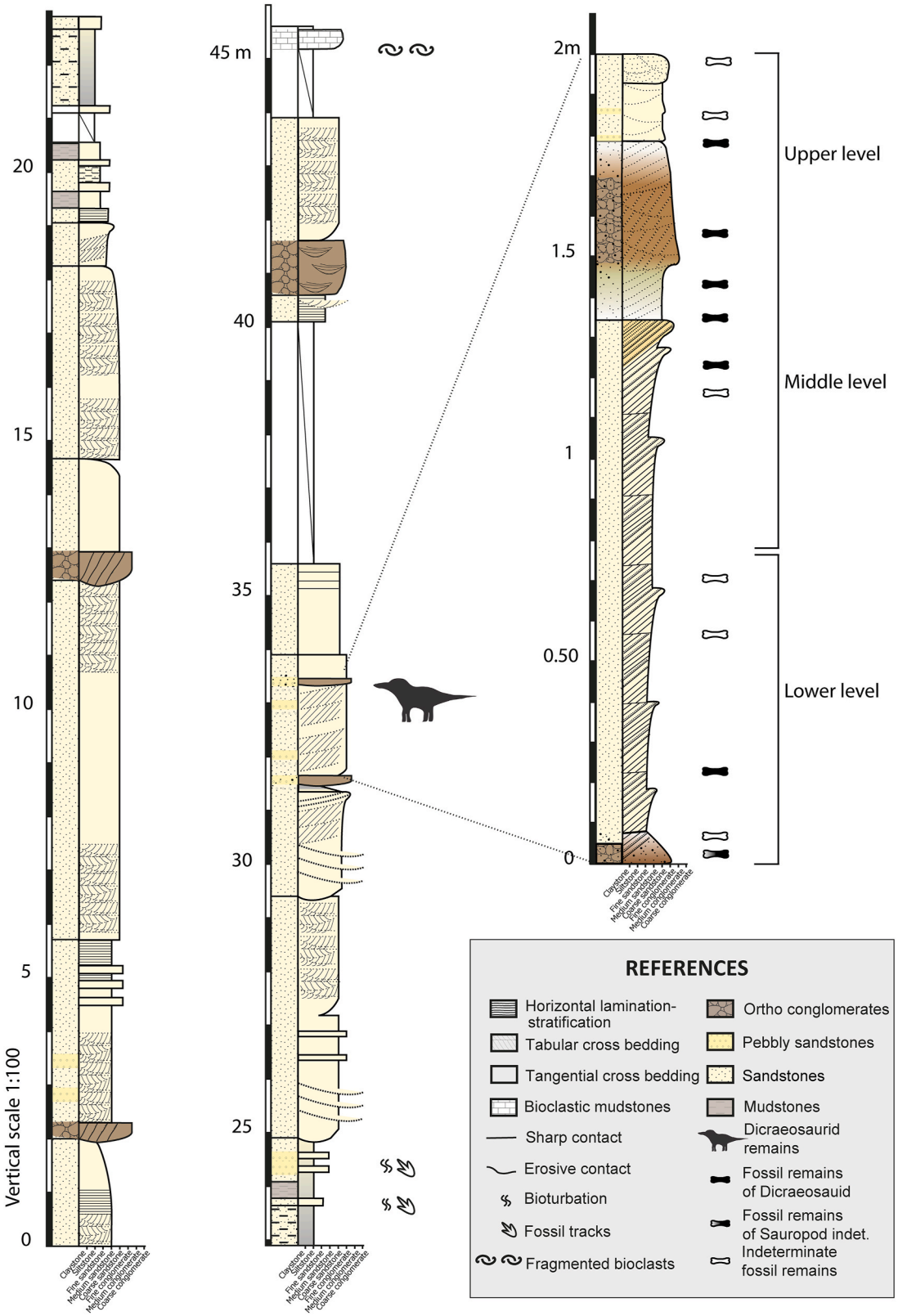

Fig. 4. Stratigraphic columns of the Mulichinco Formation showing fossiliferous levels.

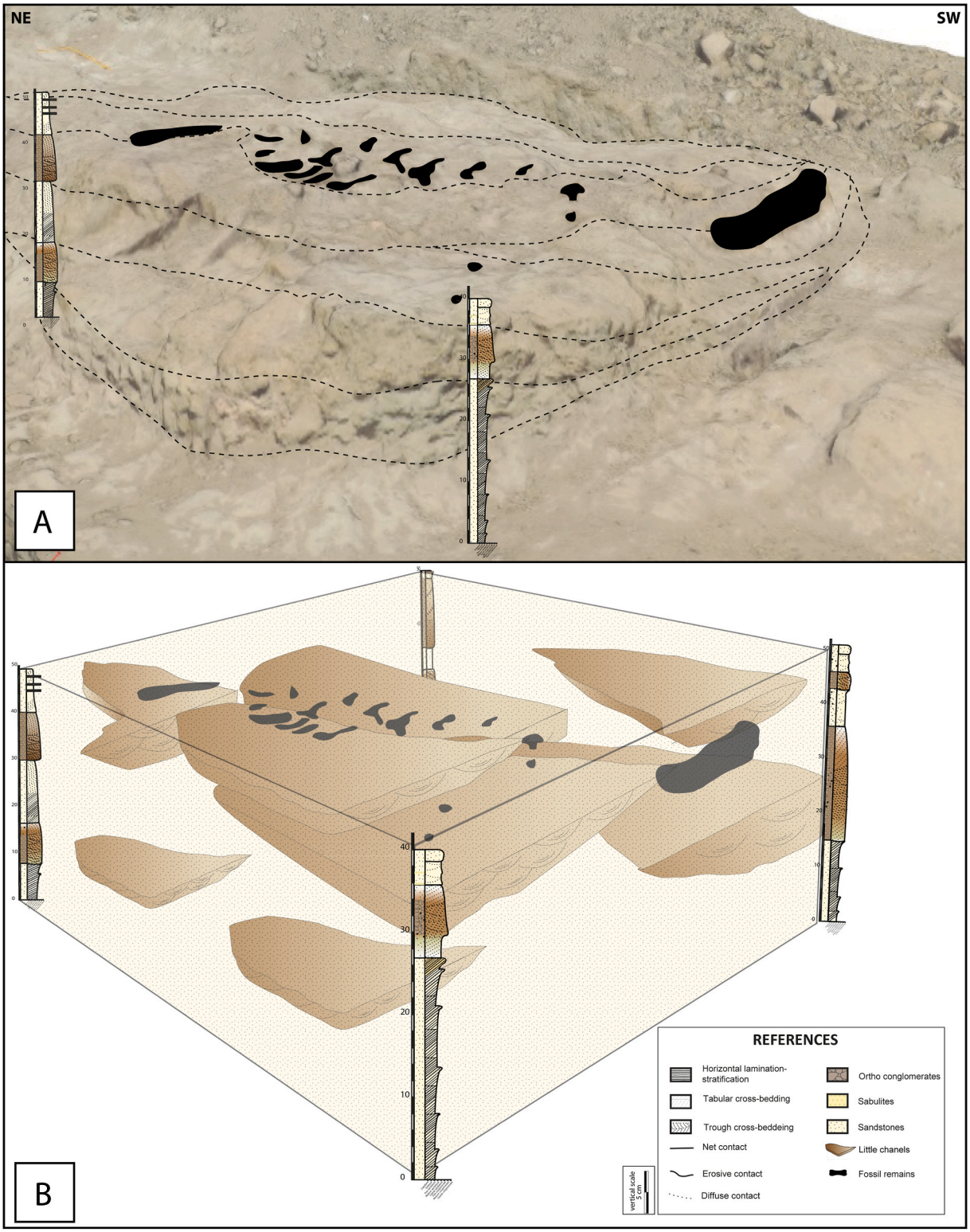

Fig. 5. 3D schematization of the spatial location of the articulated carcass and associated remains. A) 3D image with fossil remains distribution. B) Micro-profiles with detailed sub-facies and 3D reconstruction of macro-form with spatial distribution of fossil bones.

Table 1
Taphonomic characteristics evaluated for an accumulation composed of 60 bone remains from the locality of Pilmatué.

Mechanism of taphonomic alteration	Fossil remains	Percentages %
Skeletal articulation		
Semi-articulated	14	23.33%
Disarticulated associated	4	6.66%
Disarticulated not associated and very fragmented	42	70%
Weathering		
Stage 0	0	0,00%
Stage 1	31	51.67%
Stage 2	15	25%
Stage 3	2	3.33%
Absent	12	20%
Abrasion		
Stage 0	0	0%
Stage 1	39	65%
Stage 2	11	18.33%
Stage 3	0	0%
Absent	10	16.66%
Fracture		
Transverse	23	38.3%
Longitudinal	2	3.3%
Oblique	1	1.7%
Mixed	17	28.3%
Little fragment	17	28.3%
Bioerosion		
Present	2	3.33%
Absent	58	96.66%
Orientation		
Parallel/semi-parallel (articulated carcass considered a long bone was included)	19	40.42%
Perpendicular	12	25.53%
Little fossil bones	16	34.05%

Valanginian in age for the study area (Aguirre-Urreta et al., 2005). It also presents an abundant fossil records of terrestrial vertebrates (Coria et al., 2010, 2012, 2013, 2017Coria et al., 2019, 2020; Paulina Carabajal et al., 2018) and paleobotanical remains (Martínez et al., 2012; Martí nez and Olivo, 2015; Gnaedinger et al., 2017). Due to those and other regional palynological reviews (Quattrocchio et al., 2003), it is suggested a subtropical climate with seasonal dry periods as that of the prevailing climatic conditions during the deposition of the unit.

3. Institutional abbreviations

MLL-Pv, Museo Municipal de Las Lajas, Vertebrate Paleontology, Las Lajas, Neuquén Province, Argentina.

4. Materials and methods

To determine the stratigraphic position of the bone accumulation studied, a sedimentological section named “Profile of dinosaurs and plants 1" (PDyP 1) was performed. The section was measured with a Jacob stick, identifying the geometries, thickness and contacts between bodies, lithology, sedimentary structures, and fossil remains, if present (Fig. 4). Moreover, different micro-sections were measured at the site where new dinosaur bones were found, with detailed descriptions of sub-facies, granulometric variations, and body thickness (Fig. 5).

The analysis of the fossiliferous materials was carried out *in situ*. The accumulation consists of an articulated carcass that four articulated posterior cervical vertebrae with their corresponding ribs, at least four articulated posterior dorsal vertebrae with dorsal ribs in association, scapulae, and indeterminate fragments, catalogued as MLL-Pv-010. The presence of double, elongate neural spines in all vertebrae allowed identification of the specimen as the dicraeosaurid sauropod *Pilmatueia faundezi* (,Coria et al., 2019). Furthermore, a distal humeral end attributed to an indeterminate ornithopod dinosaur (MLL-Pv-018) was analyzed. All the materials commented here were found distributed within a single stratigraphic level.

From 2011 to 2019, it has been possible to excavate a continuous area on a surface of 50 square meters. Taphonomic data were collected with a graduated stick, XY axes were established from a local zero level and Z-axis was measured with a laser level. The excavation technique consists of systematic digging, recording the exact position of each finding with digital drawings and photographs. The fossil remains were documented in detail in the excavation maps based on a 1 square meter grid. Finally, the location of the bones was contrasted with an ortho-mosaic obtained from photogrammetry with Metashape PhotoScan Professional® software.

Table 2
Lithofacies recognized in the locality of Pilmatué.

Facies	Code	Lithology	Geometry	Sedimentary structures	Fossil content	Interpretation
F1	Gcm	Clast-supported conglomerate	Lenticular	Massive	Isolated fossil remains and fossil wood remains	Filling of channels with gravel-sandy load domain, forming bars deposits (Miall 1978, 1996; Smith and Edwards 1991; Nemec and Postma 1993)
F2	Gt SGt St	Conglomerates to Pebbly sandstones Coarse-grained sandstones	Lenticular bodies (sets) to tabular co-sets	Massive/Trough cross-bedding Trough cross-bedding	Isolated fossil remains	Broad shallow bodies with lag deposits and longitudinal bars (Miall 1978, 1996)
F3	St	Very coarse to coarse-grained sandstones with pebbly sandstones interbedded	Tabular	Tangential cross-bedding	Fossil vertebrate and wood remains	Sand-gravelly macro-forms formed downstream, in channels of lower hierarchy and of low depth (McCabe and Jones, 1977; Miall, 1996)
F4	Sp Sr	Coarse to medium-grained sandstones	Tabular	Planar cross-bedding Ripple marks	–	This lithofacies forms by the migration of 2-D dunes (Miall, 1996). The set of ripples at the base suggests a superimposed bedform through a reactivation surface of a low angle. These features suggest variations in the flow regime (Reesink and Bridge, 2011)
F5	Sh	Médium to fine-grained sandstones	Tabular	Horizontal bedding/ lamination	–	Flat layer deposits, a product of a variation of energy in the system towards a high flow rate (Alexander et al., 2001)
F6	Fl Fm	Very fine-grained sandstones	Tabular	Parallel lamination to ripple cross lamination, and mudcracks on the top	Invertebrate bioturbation and footprints of continental vertebrates	Deposition from suspension and from weak traction currents (Miall, 1996). Floodplain deposits, originated during processes of vertical accretion due to flooding in the system (Miall 2014)
F7	Fl	Shales with fine-grained sandstones interbedded	Tabular bodies	Parallel lamination/ Massive	–	Floodplains generated during overbank vertical accretion (Nanson and Croke, 1992; Miall 1996, 2014).

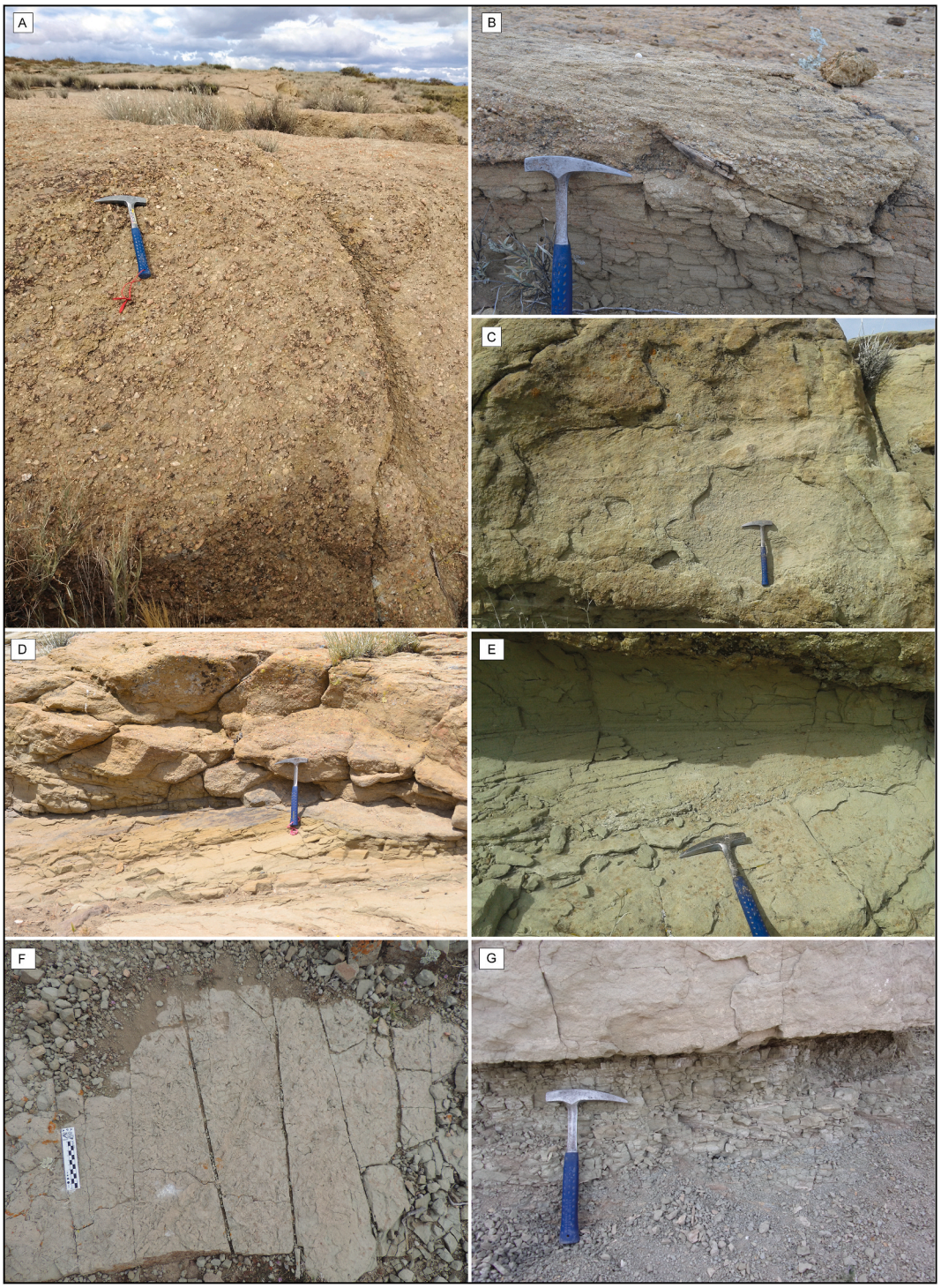

Fig. 6. Detailed photograph of facies identified in the studied area. A. massive clast-supported conglomerate with sandy matrix (F1). B. pebbly sandstones with interbedded coarse-grained sandstones. Note the undetermined fossil fragment concordant with the stratification planes (F2). C. coarse to medium-grained sandstones with planar cross-bedding (F3). D. very coarse to coarse-grained sandstones with cross-bedding (F4). E. medium-grained sandstones with cross-stratification from a low angle to parallel stratification towards to the top (F5). F. very fine-grained sandstones with invertebrate bioturbation and footprints of continental vertebrates (F6). G. shales with parallel lamination (F7).

The following taphonomic alteration mechanisms were contemplated:

Skeletal articulation. This feature was evaluated according to the stages proposed by Behrensmeyer (1991); articulated, disarticulated but associated, and disarticulated dispersed and isolated.

Weathering degree. The following categories proposed by Fiorillo (1988) were contemplated for fossil remains: 1- intact remains; 2- remains showing/with surface loss of bone material; and 3- remains with significant loss of bone material.

Abrasion degree. This alteration mechanism was determined following the categories reported by Fiorillo (1988): 0- remains showing surface intact; 1- bone with rounded edges and polished; 2- bone with moderate polish and well-rounded edges; and 3- bone with all very well rounded edges and well-polished surface.

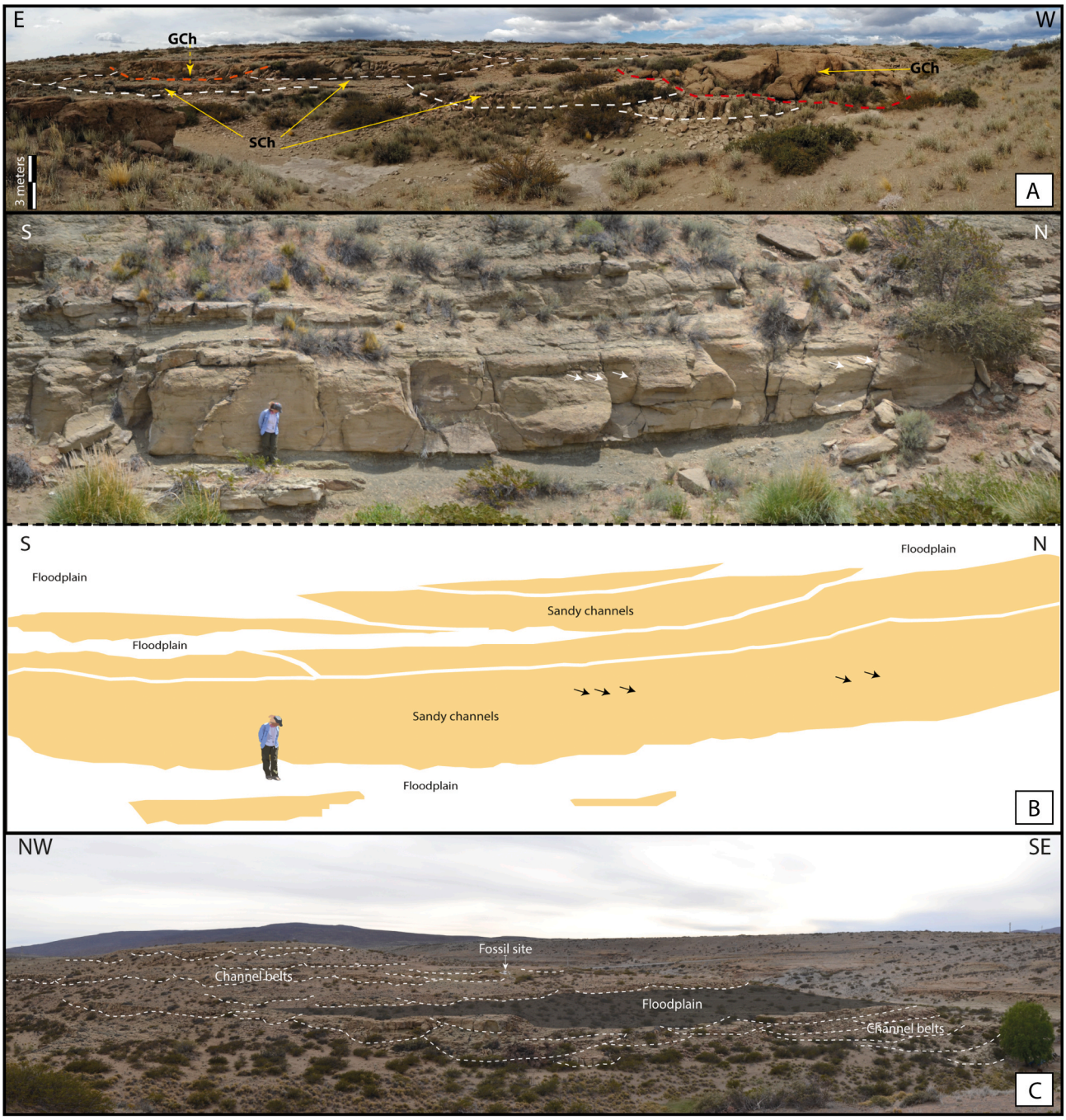

Fig. 7. Facies associations. A. sandy gravel channels (GCh) associated with sandy channels (SCh) vertically and in their adjacencies. B. photograph and interpretation of sandy channels belt with scarce preservation of floodplain. The direction of migration of the bars is indicated with arrows. C. relationship of the channels with the flood plain. Note how the channels amalgamate into a belt.

Breakage. This attribute was determined following the scheme of Casal et al. (2013). The types of fractures were measured in bones with lengths greater than 8 cm, considering the angle formed between the proximal-distal major axis and the fracture. Longitudinal, transverse, oblique and mixed fractures were thus recognized.

Bioerosion degree. This attribute was determined considering the presence or absence of bone surface breakdown made by organisms (Casal et al., 2013).

Transport and orientation. This taphonomic attribute was estimated considering the distribution of the fossil set, related to the proposal made by Voorhies (1969) and Todd and Frison (1986).

The recognized attributes were observed *in situ* during fieldwork and organized in a table of taphonomic attributes (Table 1), which was processed and plotted in a taphonomic map.

5. Results

5.1. Facies associations

The outcrops of the Mulichinco Formation have great lateral continuity. This formation shows a reduced thickness that reaches ~45 m. The section allowed recognizing seven sedimentary facies (F1 to F7) that constitute the three facies associations described below. The facies are arranged in a fining-upward cyclic sequence, from fine conglomerates to

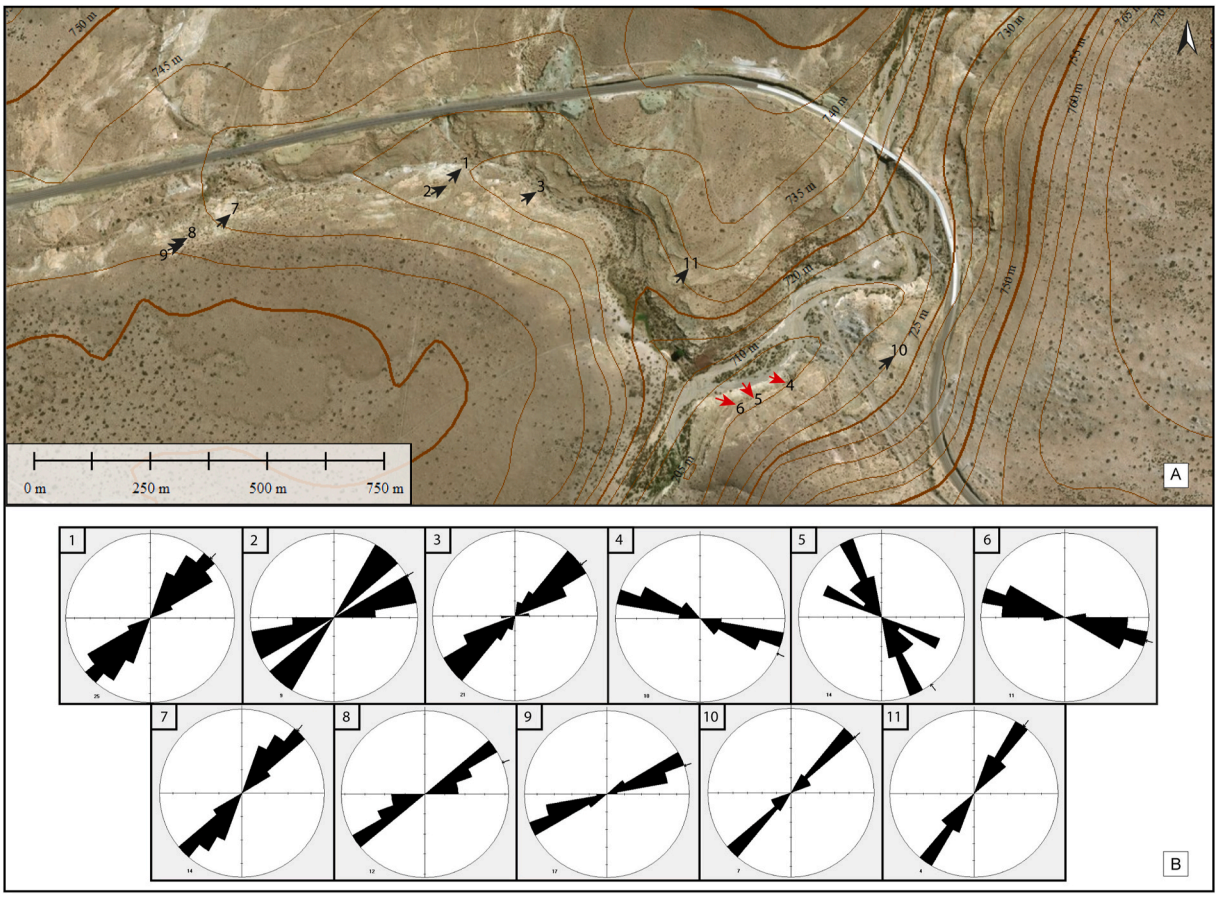

Fig. 8. Satellite image from Google Earth showing the paleocurrent directions for the study area. These include 132 readings taken from fluvial deposits of the Mulichinco Formation. A. local paleocurrent patterns. Note the paleocurrents predominance towards the northeast. B. rose diagrams, corresponding to each measurement station. The number of paleocurrent in each station is expressed in the lower left margin.

medium to fine-grained sandstones that pass to very fine-grained sandstones and shales. Properties and interpretation are shown in Table 2, and main features in Fig. 6.

Three facies associations of continental origin were established as having developed in distal gravelly rivers. To group the facies, we considered the geometry, lithology, primary structures, fossil content and the relationship between the rock bodies. In this sense, the F1 and F2 facies, with predominant fine conglomerates (Gcm or Gt + SGt or St) were grouped into FA 1; the facies F3, F4, and F5, with pebbles and predominance of coarse to medium-grained sandstones (SP + Sr or St or Sh) were grouped into FA 2; and facies F6 and F7 characterized by massive to laminated very fine-grained sandstones to shales (Fl + Fm or Fl) were grouped into FA 3 (Fig. 7).

5.1.1. *Facies association 1*

This facies association is composed of lenticular bodies with an erosive base and a fining-upward general arrangement. From base to top, this association comprises clast-supported conglomerates with a coarse-grained sandy matrix, in bodies of 2 m thick, followed by coarse to medium-grained sandstones with trough cross-bedding. These bodies include several fining-upward cycles of variable thickness (0.4–0.6 m), limited by erosional surfaces and grouped into co-sets of 1.5–2 m thick. Towards the top, they present medium-grained sandstones with trough cross-bedding, arranged in sets of 0.4 m thick, forming 1.3 m thick co-sets. Paleocurrent orientations measured in these sandstones suggest prevailing currents flowing towards NNE (Fig. 7A).

5.1.2. *Facies association 2*

This association consists of sets of lenticular beds with erosive base and variable thickness (2–2.5 m) that form co-sets of tabular geometries. These comprise a succession of massive fine conglomerates and coarse-grained sandstones with tangential cross-bedding. Sporadically, these bodies are laterally associated with gravelly channels; in other cases, they are associated with floodplain deposits (Fig. 7B). This association exhibits isolated and disarticulated fossil remains into the pebble lags, in addition to abundant vertebrate fossil remains (articulated carcass with associated isolated bones) immersed in medium to coarse-grained sandstone with fine-conglomerates interbedded. The vertical succession ends up with tangential cross-bedding sandstones of low angle, sometimes, with horizontal stratification.

5.1.3. *Facies association 3*

This association presents tabular bodies with clear bases made up of a succession of massive or, sporadically, of laminate shales interbedded with very fine-grained sandstones. These bodies show variable thickness and scarce lateral extension (Fig. 7C). Towards the top, invertebrate bioturbation and vertebrate footprints attributed to dinosaurs were found to be associated with mud cracks and symmetrical ripples

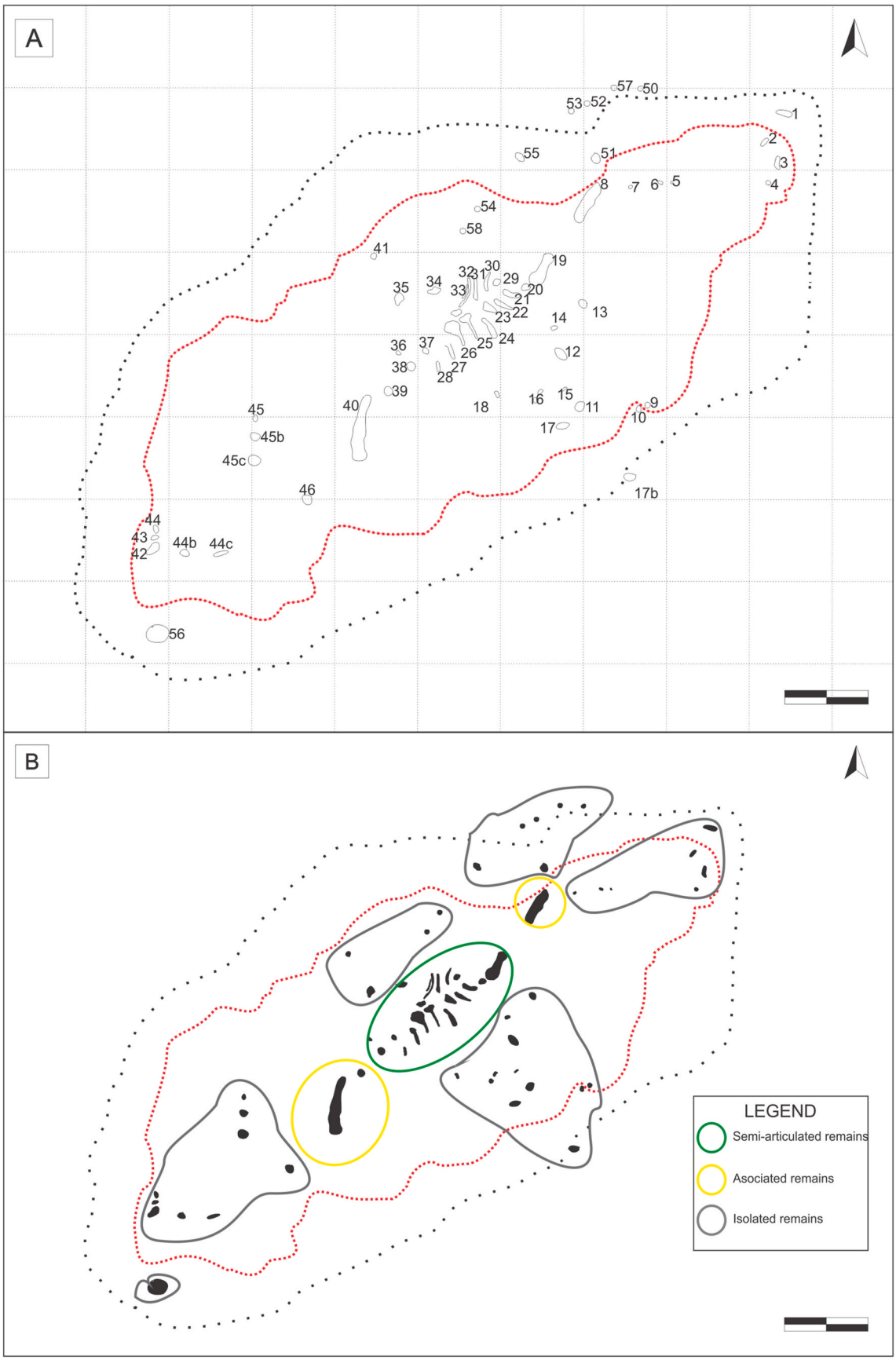

Fig. 9. Taphonomic maps and grouping of bone remains. A. taphonomic map with the location and numbering of the fossil remains. B. grouping of remains according to the categories of articulated carcass, associated remains and isolated non-associated remains. Scale bar: 1 m.

Table 3
Recognizable bone elements and levels they were found.

Number	Recognizable bone elements	Skeletal articulation	Weathering	Abrasion	Fractures	Level
20	Neural spine	Articulated	1	1	Transverse	Upper
21	Neural spine	Articulated	2	1	Transverse/longitudinal	Upper
22	Neural spine	Articulated	2	1	Transverse/longitudinal	Upper
23	Neural spine	Articulated	2	1	Transverse	Upper
24	Neural spine	Articulated	2	2	Transverse	Upper
25	Neural spine	Articulated	2	1	Transverse	Upper
26	Neural spine	Articulated	1	1	Transverse/oblique	Upper
27	Neural spine	Articulated	1	1	Transverse	Upper
29	Ribs?	Articulated	1	1	Transverse	Upper
30	Ribs	Articulated	1	1	Transverse/oblique	Upper
31	Ribs	Articulated	1	1	Transverse	Upper
32	Ribs	Articulated	2	1	Transverse	Upper
33	Ribs	Articulated	1	1	Transverse/oblique	Upper
40	Scapulae	Associated	2	2	Transverse/longitudinal	Middle
46	Ribs?	Associated	1	1	Transverse	Middle
56	Distal humeral end	Disarticulated and unassociated fossil remains	3	2	–	Lower
58	Vetrebrae	Associated	1	1	–	Middle

stabilized by microbial mats.

5.2. Paleocurrent analyses

Paleocurrent directions were measured in cross-bedded structures developed in coarse-grained sandstones with interbedded fine conglomerates. One hundred and thirty-two data points at eleven sites distributed throughout the study area (Fig. 8A) were measured following height values ranging from 725 to 735 m above sea level. The paleocurrent analysis indicates a SW-NE direction and a preferential sense towards the NE, with an average azimuthal value of 54° N. However, in three sectors the paleocurrents indicate a SE-NW direction. This sector was interpreted as crevasse splay deposits (Fig. 8B).

5.3. Taphonomy

The analyzed skeletal record consists of postcranial and indeterminate remains composed of 60 bones (Fig. 9A), distributed in a tabular bed with an erosive base of 3 m thick and 50 m laterally, and consisting of coarse-grained sandstones with interbedded fine conglomerates and tangential cross-bedding. The taphonomic parameters include information on fossil assemblage, general orientation, and spatial distribution of remains.

5.3.1. Skeletal articulation

The skeletal articulation was analyzed considering whether bones were found articulated, disarticulated but associated, or disarticulated and isolated (Fig. 9B). In this sense, and as previously mentioned, three main levels with vertebrate fossil remains distributed in the sandy horizon were recognized. (a) The lower interval contains disarticulated and unassociated fossil remains, consisting of indeterminate highly fragmented skeletal elements (20% of the total). These remains are included in fine conglomerates with very coarse-grained sandstone matrix. (b) The middle interval encompasses remains associated with the main carcass and fragmented bone remains. Here, there are long bones and bone fragments with a clear major axis, such as tendon, and rib fragments (23.33% of the total). These are immersed in well-classified coarse-grained sandstones. (c) The upper interval encloses an articulated carcass consisting of ribs, posterior cervical and dorsal vertebrae, and neural spines, and indeterminate fragmented bones (56.66% of the total bones recovered) (Table 3). These skeletal remains are submerged in coarse to very coarse-grained sandstones, partially covered by well-selected polymictic conglomerates (Fig. 10A)

5.3.2. Weathering degree

The recognized degree of weathering varies between 1 and 3, following Fiorillo (1988). In this sense, 51.67% of the remains have weathering grade 1 (31 remains), 25% have grade 2 (Fig. 10B) (15 remains), and the rest (20%) are fragmented to the point that attributes could not be estimated (12 remains). Only two bones (a distal humeral end attributed to an indeterminate Ornithopoda and another indeterminate bone fragment) have grade 3 (3.33%) (Fig. 10C), these bones were found in the basal section in contact with fine deposits of the flood plain and at the top of the section, respectively (Fig. 11A).

5.3.3. Abrasion degree

The articulated remains are interbedded in fine conglomerates and present mild abrasion with softened edges (stage 1, 65%, 39 remains of the total) (Fig. 10D). The non-associated scattered bones, immersed in coarse to medium-grained sandstones show a moderate abrasion with pronounced polishing, with ends and edges well rounded (stage 2, 18.33%, 11 remains of the total) (Fig. 10E). The rest of the bones (10 remains of the total) represent 16.66% of the boneset, exposing only a small section of bone. Therefore, we could not measure this attribute (Fig. 11B).

5.3.4. Breakage

Regarding integrity, 61.67% are complete and retain the relative anatomical position, and the remaining 38.33% are isolated and broken. The analysis of breakage indicates that transverse fractures were most abundant (38.3%) (Fig. 10D), followed by combined fractures (28.3%) and longitudinal ones (3.3%), whereas oblique fractures (1.7%) were much less frequent. The remaining 28.3% are little fragments, and diagnostic signs for fracture were not identified. Host rock and fossil remains are affected by brittle deformation with fractures with NNE-SSO orientation (Fig. 12A).

5.3.5. Bioerosion

Two types of trace of bioerosion were identified. On one hand, there is a partially preserved conical trace in the isolated bone (MLL-Pv-018), tentatively attributed to a tooth mark which was identified on the right side of the ventral view (Fig. 12B). On the other hand, circular

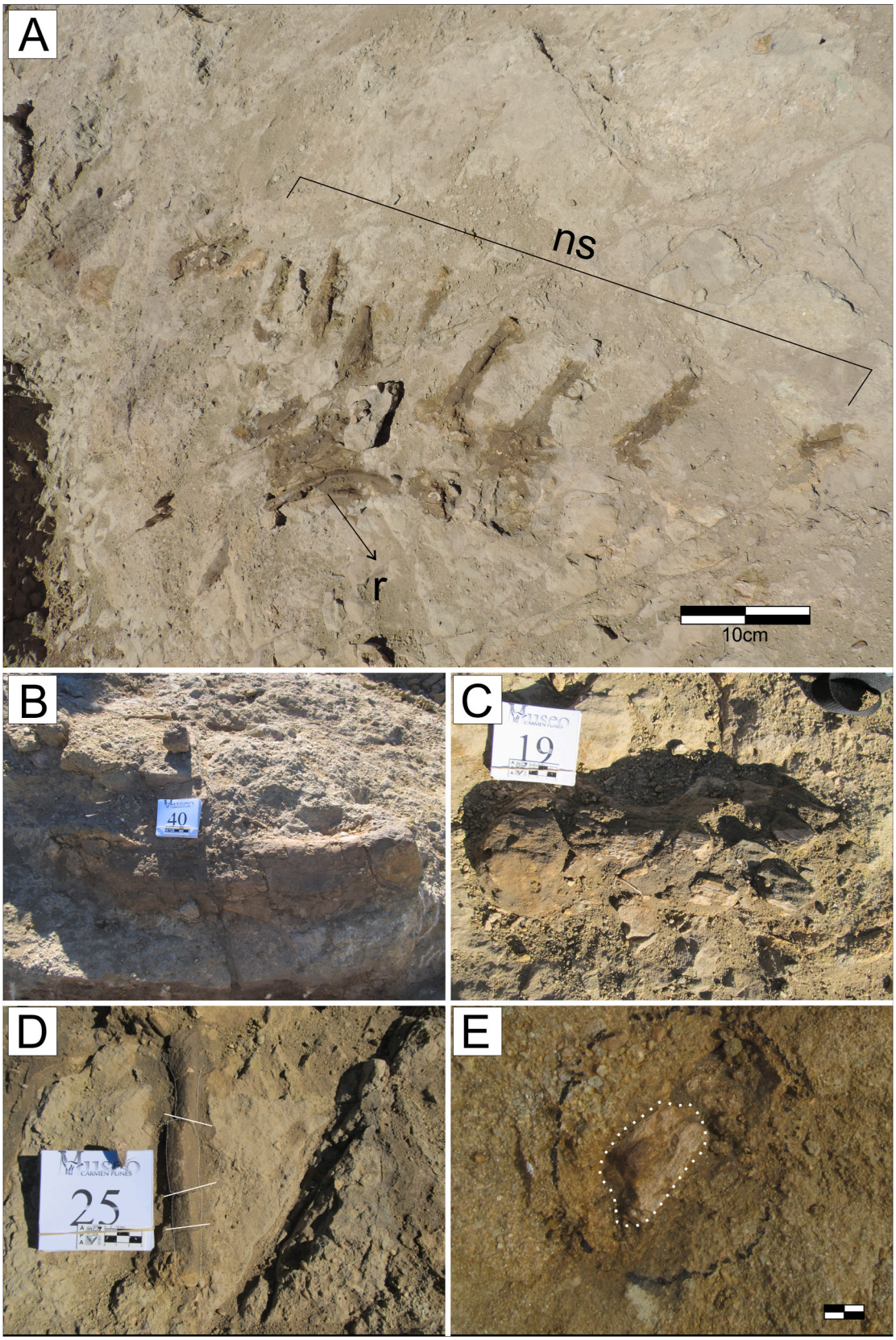

Fig. 10. Articulated carcass and bone remains catalogued as MLL-Pv-010. A. articulated sequence of neural spines with ribs in anatomical position and indeterminate bone non-associated. B. Scapulae with weathering degree 2 to 3. C. indeterminate bone with weathering degree 3. D. neural spine with abrasion degree 1 and weathering degree 2. Note the transverse fractures. E. indeterminate bone fragment with abrasion degree 2. Abbreviations: ns, neural spines; r, ribs. Scale bar in E: 3 cm.

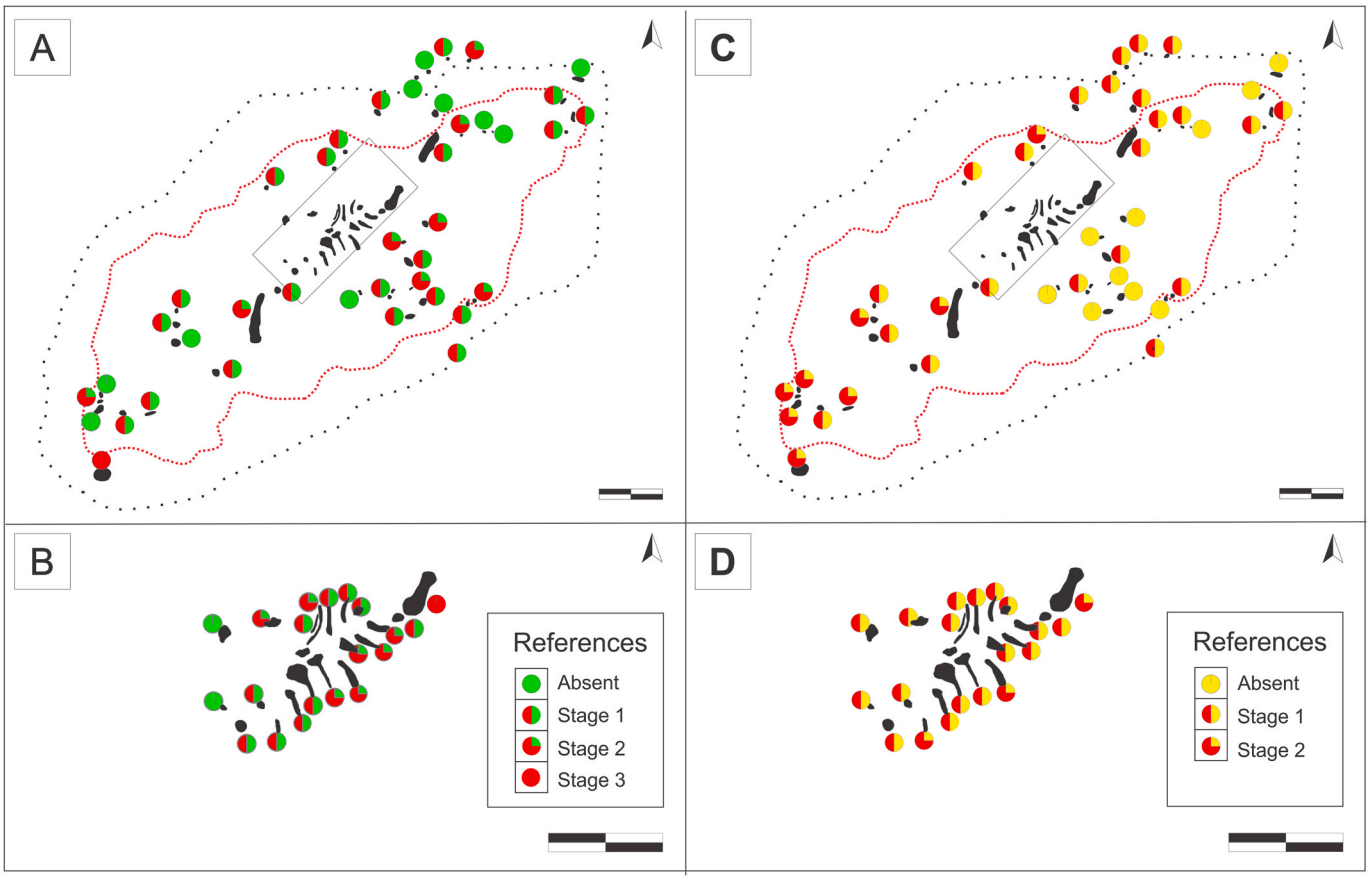

Fig. 11. Schematic maps of taphonomic attributes. A. weathering map according to stages proposed by Fiorillo (1988). B. detailed weathering stages of the articulated carcass. C. abrasion map according to stages proposed by Fiorillo (1988). D. detailed abrasion stages of the articulated carcass. Scale bar: 1 m.

bioerosion marks compatible with traces of invertebrates were identified, in the indeterminate element n°19, protected as a constituent element of the MLL-Pv-010, penetrating the spongy tissue (Fig. 12B). For both cases, it was not possible to determine the organism that produced the bioerosion marks.

5.3.6. Orientation

The orientation analysis shows that 40.42% of the long bones are oriented parallel or sub parallel to the main flow. In this group, the main carcass (composed of 13 articulated bones) was included and considered a long bone. 25.53% are oriented perpendicular or sub-perpendicular to the main flow, and the rest (34.05%) were very fragmented, so their orientations could not be determined (Fig. 12C).

6. Discussion

Facies association suggests that accumulation developed in a braided fluvial system, due to the recognized stacking pattern, the development of channel belts, and the scarce preserved floodplain (Fig. 13). From the analysis of the facies association, three sub-environments in the system were determined: minor channel fill, low-sinuosity channel system, and muddy-sandy floodplain. The minor channel fills were dominated by the formation and migration downstream that formed lagged deposits and longitudinal bars generated in a shallow, low flow regime (Miall, 1978, 1996, 2014; Smith and Edwards, 1991; Nemec and Postma, 1993). In the low-sinuosity channel system, the traction structures recognized are interpreted as mega-dune migration, which would allow the generation of compound bars. This process indicates that the channels were active for a prolonged period. Internally these bars present levels with unidirectional ripples and low-angle reactivation surfaces. The development of small lentiform bodies that erode the bars would have been generated between the fluctuations of flow energy and flood events, which allowed the removal of vertebrate remains upstream, and their transfer to run around in these forms of bed, burying them quickly and creating a fossil site (Coria et al., 2010, 2012, 2013, 2017, 2019, 2020; Gnaedinger et al., 2017; Paulina-Carabajal et al., 2018). In this sense, the micro-profiles allowed us to recognize the depositional dynamics within a longitudinal bar in which three levels with fossil bones distributed in 2-m thickness section were identified (Fig. 14). Finally, the floodplain deposits resulted from the flooding processes and the influence of the water table that facilitated the occasional development of small bodies of shallow water. This process indicates that the plain did not have good drainage, which favored their development. Fluctuations in the water column were common, sometimes with exposure evidenced by the presence of mud-cracks. The duration of these water bodies allowed, in turn, the development of biogenic activity, recognized by the traces of invertebrates and of large vertebrates. The latter probably used them as sources of water and took advantage of low-level setting to establish places of transit. The interbedded sandy levels are interpreted as overflow deposits with rapid invertebrate colonization.

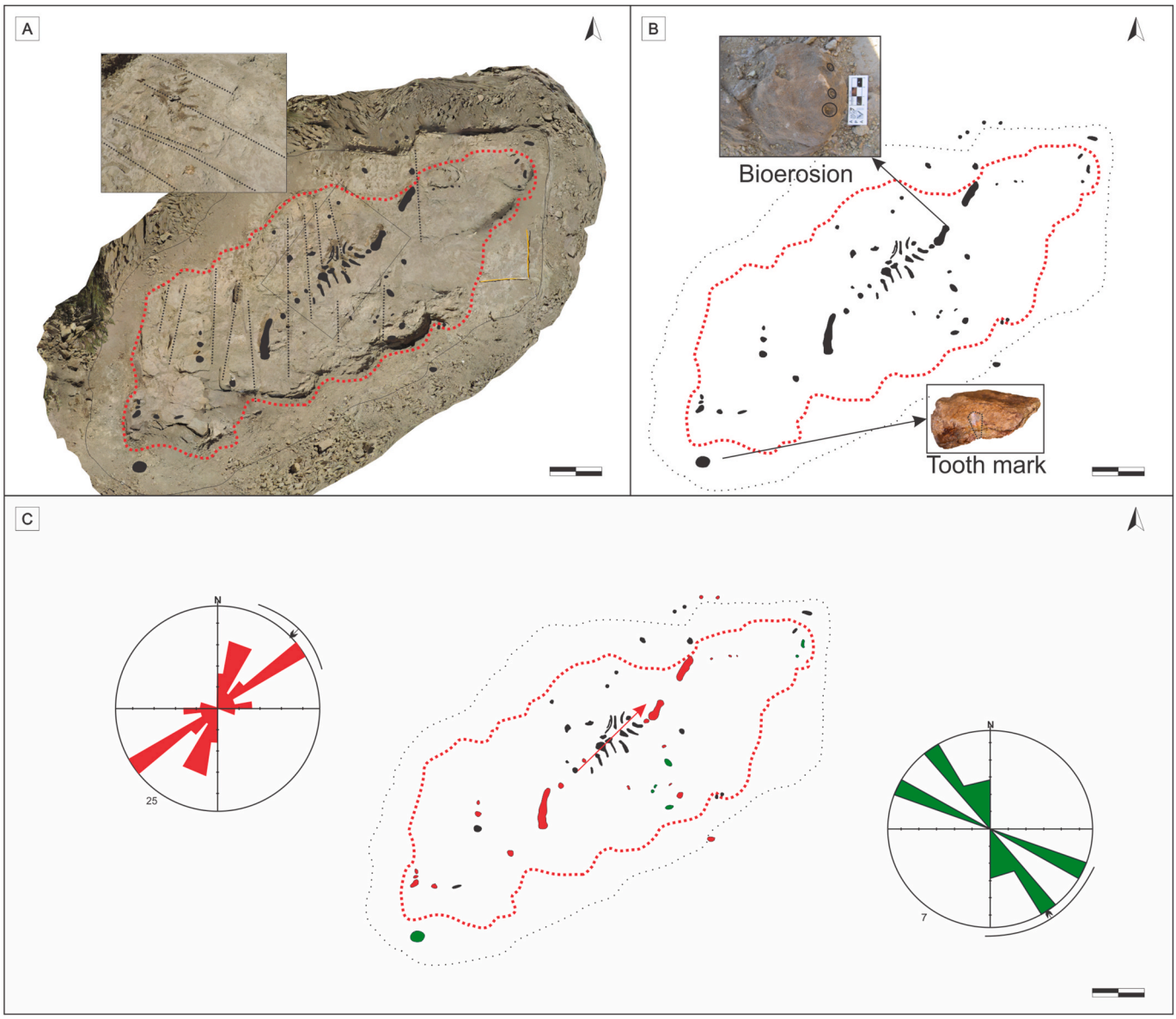

Fig. 12. Schematic maps of taphonomic attributes. A. fragile deformation that affects the fossil site and some fossil remains. B. detail of bioerosion marks in two non-associated bones. C. orientation diagrams of the long bones.

According to the results, the fossil assemblagewas accumulated in a sandy gravel macro-form developed downstream, in channels of lower hierarchy and low depth (McCabe and Jones, 1977; Miall, 1996).

The final spatial configuration of the fossil assembly can be explained from the biostratinomic processes, such as the disarticulation, transport, and reworking that took place immediately after death until its final burial (Fig. 15).

The disarticulation can be related to three factors: type of joint (synovial, cartilaginous, and fibrous), type of environment, and action of predators and/or scavengers (Araujo Junior and Bissaro Junior, 2017). The synovial joints are generally the first to disarticulate, which would explain the absence of some parts of the skeleton. In this sense, following the sequence of disarticulation proposed by Hill (1979); Hill and Behrensmeyer (1984); Lyman (1994) and considering the articulated bone remains, we can infer that the appendicular bones were the first to disarticulate, the scapula and the coracoid dispersed away but remained associated and immersed in a level below the main carcass. On the other hand, cartilaginous joints tend to hold longer the skeleton together, which would have allowed articulated transport of the remains.

Moreover, the climatic conditions would also have played an important role in these processes. For instance, Martí nez and Olivo (2015) proposed a warm climate with dry seasons during the deposition of the Mulichinco Formation (Fig. 16), and seasonal variations favor the disarticulation processes (Todd 1983). Finally, except in the distal humeral end and in an indeterminate bone (Fig. 12B), we have not recognized the action of scavengers and/or predators in the rest of the bone assembly; yet such action cannot be ruled out.

The estimated degree of weathering shows similarities in the middle and upper levels (1 and 2°, respectively). The presence of articulated remains and their integrity indicate that the time of exposure to the weather was not long. However, at the lower level, weathering is accentuated to grade 2 to 3. This level has indeterminate and highly fragmented remains; hence, we can infer that they were exposed to weathering agents for a longer time. Regarding abrasion processes, grade 2 abrasion predominates at the lower level. These remains have sub-rounded edges and a pronounced polishing; we contemplate that this alteration process was generated during transport and after the fracture. On the other hand, both at the middle and upper levels, degrees

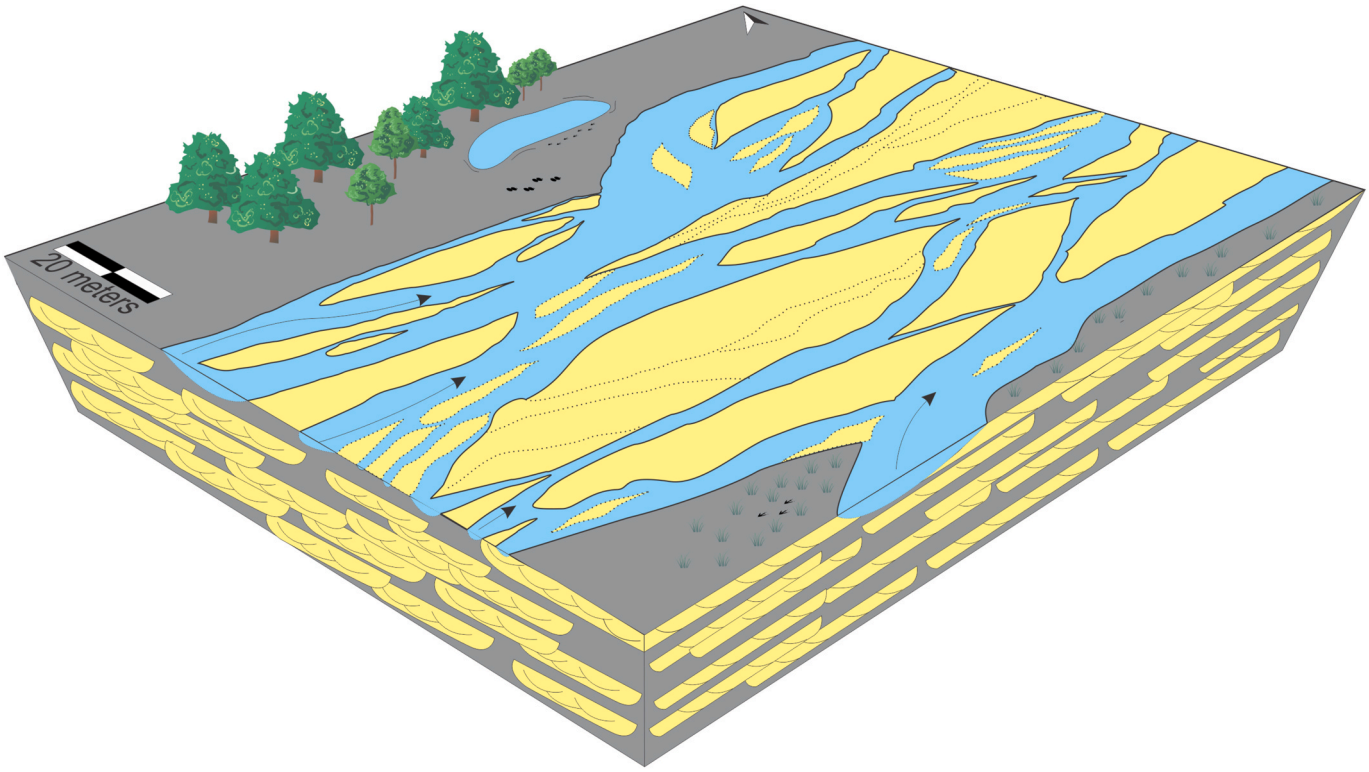

Fig. 13. Interpretation of braided fluvial system predominant in the study area.

of abrasion of 0–1 were recognized. We consider that at the time of transport, the carcass retained the soft tissue that allowed it to maintain its integrity, which would have minimized the low or early rounding of the remains (Fernández Jalvo and Andrews, 2003; Casal et al., 2013). In the entire sample, the same fracture patterns have been identified, indicating that they have been able to go through biostratinomic (3.3% longitudinal fractures) and diagenetic processes (combined and transverse fractures, 28.3% and 38.3%, respectively) as well (Shipman et al., 1981; Alcalá, 1994; Alcala and Escorza, 1998). The prevalence of diagenetic rupture processes over biostratinomic rupture processes is worth noting.

The spatial disposition of bone remains indicates that they were dispersed by the action of an unidirectional aqueous flow, with an orientation predominantly to the northeast. The analysis of the orientation indicates that most bone remains are parallel or semi-parallel to the direction of the paleocurrent and only a small group is perpendicular to the main flow direction (Fig. 12C). Therefore, we can infer that the remains whose arrangements are parallel were mobilized in the section of the channel with greater flow, and the orthogonal remains could be associated with energy fluctuations that favored their rework and relocation. The action of an aqueous flow produces the first bone concentration and downstream, it will generate secondary concentrations consisting of several elements and individuals (Hill, 1979). Physical transport by an aqueous stream can cause selective removal and accumulation of certain bone elements (Norman, 1987; Wood et al., 1988; Lyman, 1994; Martin, 1999 cited in Noto, 2011). The presence of an incomplete but articulated carcass with associated dispersed bone remains would suggest that were sorted from a nearby location and latter arrived to its final accumulation zone.

Many authors studied the behavior of bone remains during transport in fluvial systems (Voorhies, 1969; Behrensmeyer, 1975; Todd and Frison, 1986) and established a transportability order related to the geometry of the bones and the buoyancy capacity of each type of bone. In this sense, Todd and Frison (1986) estimated, through experimental studies, the Fluvial Transportation Index (FTI) for elephant bones. Its comparison with that of the groups reported by Voorhies (1969), showed similar results (see Lyman, 1994 and references in this regard). According to these studies, the group of bones analyzed presents FTI values (Table 4) that indicate that the accumulation and dispersion of fragmented bones at the lower level is related to the general morphology of these remains, which favored transport by rolled or saltation in contact with the bottom of the canal. This type of transport causes marked wear of the fractured ends.

By contrast, accumulation at the upper level was favored by the high FTI of the main carcass and associated bone remains, which would have allowed rapid transport, fluctuating in the water column in occasional contact with the bottom of the channel. The transport of these skeletal remains with soft tissues is still present and the rapid burial would have favored their preservation. Therefore, considering the bone remains present in the accumulation, we infer that it is represented by a multispecific assemblage with bone remains from different origin areas. Although the main carcass represents 26.6% of the total, the indeterminate remains indicate a possible mixture of individuals. Also, the different taphonomic attributes recognized in the various bones indicate different conditions and times of transport.

7. Conclusions

- The facies association indicates is the presence of a braided type fluvial system with amalgamated channels, longitudinal and a

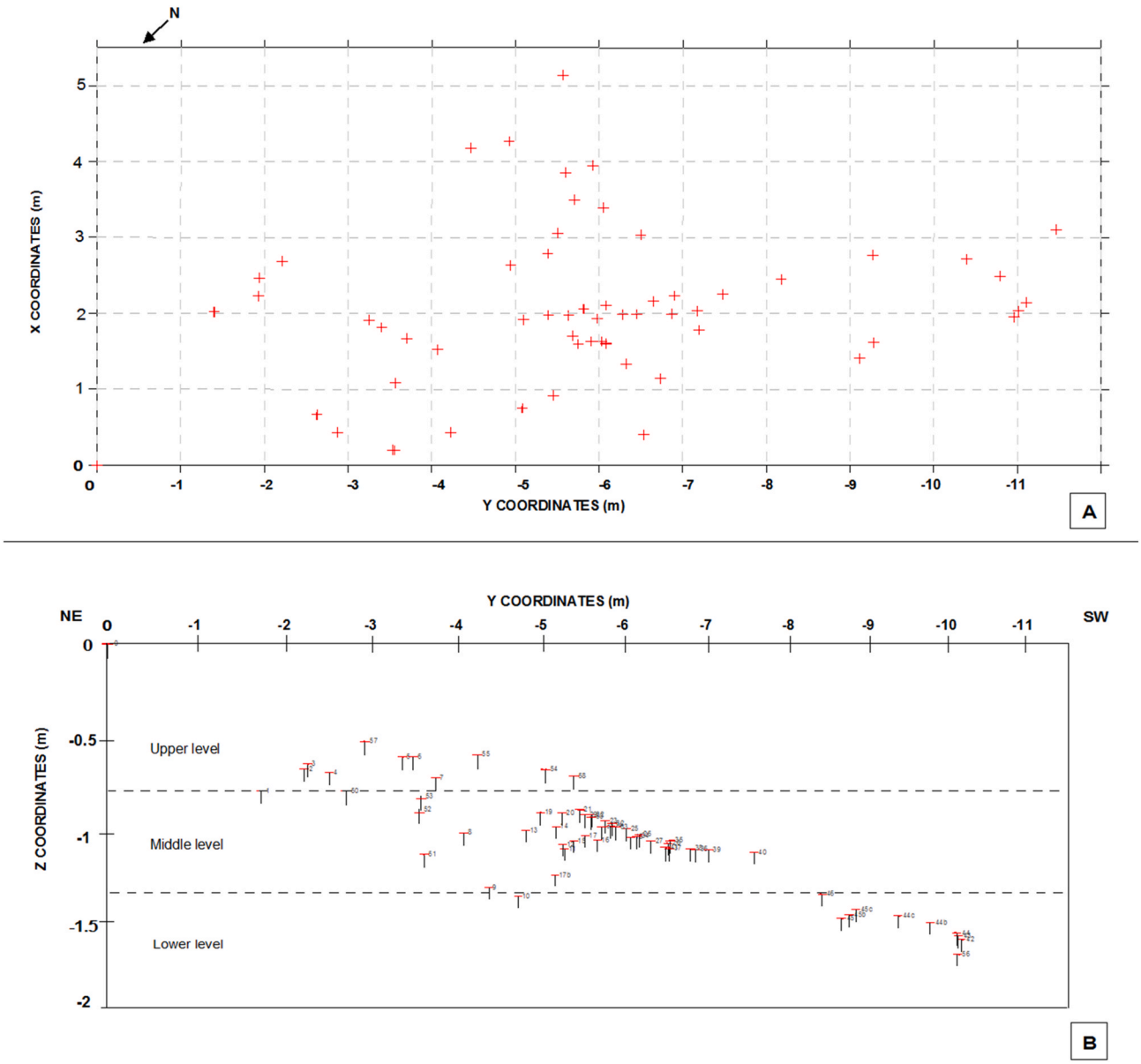

Fig. 14. Spatial distribution of fossil remains. A. spatial distribution (X–Y plane) of skeletal elements. B. spatial distribution of skeletal elements in Y-Z section, with three fossil-rich levels with different taphonomic attributes (see text for further explanation).

transverse bars, and scarce development and preservation of floodplain. These results provide information for the southern sector and complete previous regional studies on the southernmost outcrops of the Mulichinco Formation.

- The paleocurrent analysis indicates a flow with a southwest-northeast direction with a predominantly northeast sense (N54° E), where the source areas are located to the south, south-west and to west.
- The analyzed fossil accumulation was the product of dispersion through physical aqueous processes and was preserved in a longitudinal bar deposit.
- From the micro-profile analysis, three levels with bones were determined in the accumulation.
- The selective transport and taphonomic attributes that characterize the bone remains indicate that the fossil assemblage is the result of an accumulation of different origins.
- The taphonomic attributes allowed establishing two associations from the three levels of bone remains formed during different events. The lower level is the result of the pebble lags where indeterminate fragments having taphonomic characteristics that indicate fragmentation followed by transport were accumulated. The middle and upper levels show a different biostratinomic history that suggests close generation with the presence soft tissue allowed maintaining the integrity during transport.
- The taphonomic attributes identified at the lower level allow us to infer a combination of easily transportable elements, probably of regional origin.

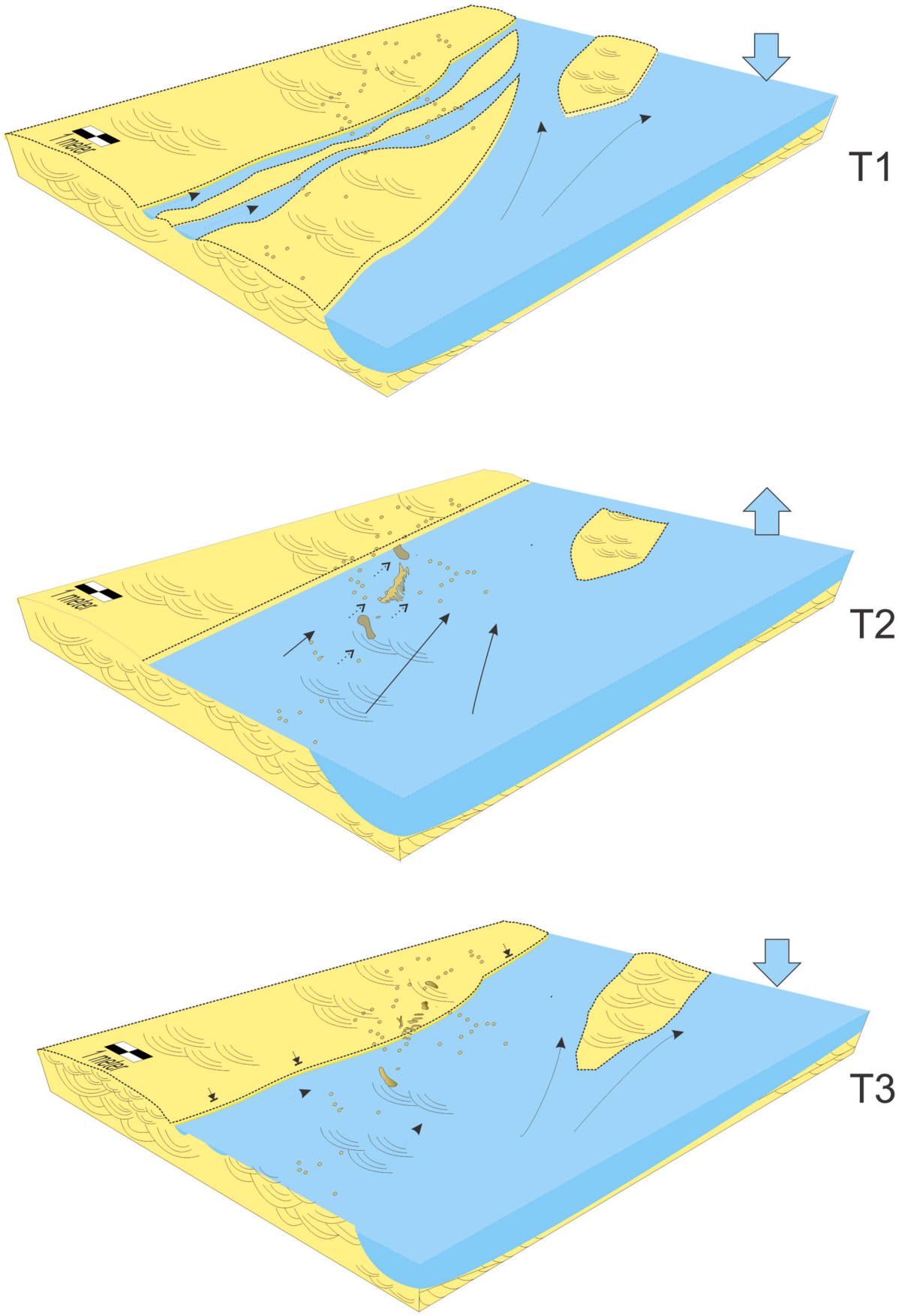

Fig. 15. Schematic interpretation of the energy fluctuations of the system and the arrival of the fossil remains at the accumulation site (T: Time).

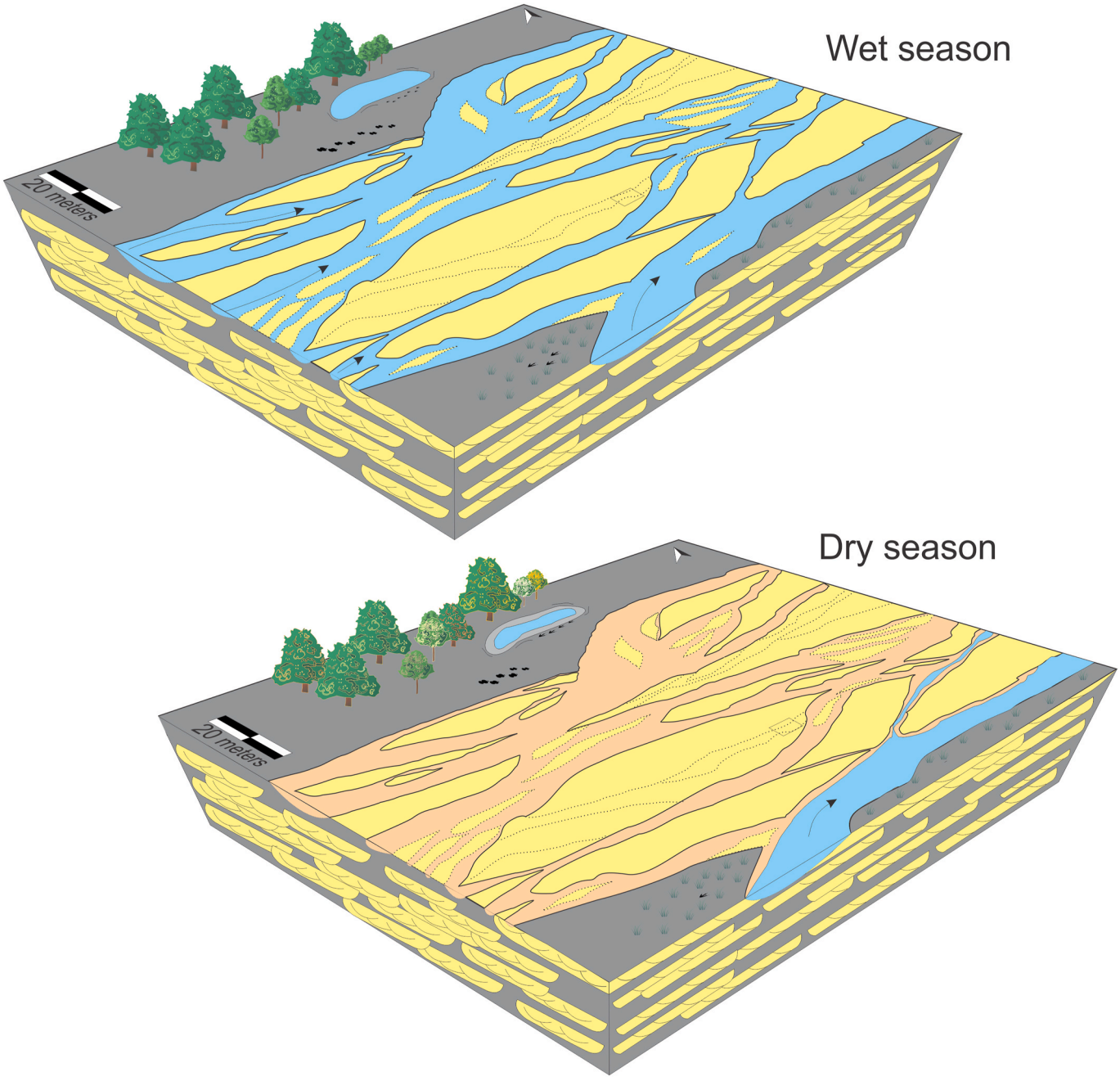

Fig. 16. Interpretation of paleoenvironment variations according to the climatic variations inferred during Mulichinco Formation deposition.

Table 4
Fluvial Transportation Index (FTI) values for the bone remains found in the locality of Pilmatué, following the proposal of Todd and Frisson (1986). Values higher than 75 indicate high susceptibility to transport, values between 50 and 74 denote moderate susceptibility to transport, and less than 50 shows resistance to transport.

Skeletal elements	FTI
Caudal Vertebra	92.43
Cervical vertebra	96.64
Dorsal Vertebra	76.43
Ribs	53.98
Scapula	62.95
Femur	24.26

- The taphonomic attributes observed at the middle and upper levels in the largest and most complete specimens allow us to conclude a parautochthonous origin, although without significant transport.
- The set of fossil bones constitutes a multispecific accumulation of bones identified as a dicraeosaurid sauropod (middle and upper levels) to an indeterminate ornithopod and several remains with no taxonomic identification (lower level).

CRediT authorship contribution statement

Diego A. Pino: Data curation, Writing - original draft, Writing - review & editing. **Rodolfo A. Coria:** Supervision, Writing - review & editing. **Ignacio Díaz-Martínez:** Supervision, Writing - review & editing. **Maisa A. Tunik:** Supervision, Writing - review & editing.

Declaration of competing interest

The authors declare that they have no known competing financial interests or personal relationships that could have appeared to influence the work reported in this paper.

Acknowledgments

We thank the team of professionals F. Bellardini, M. Baiano and G. Windholz and staff of the Carmen Funes Municipal Museum of Plaza Huincul and, particularly, to the staff of the Las Lajas Museum, Ramón Faúndez and Pablo Sandoval for their work and assistance in the field. We are also grateful to Manuela Zalazar and Ricardo Gómez for the critical reading of a preliminary version of the manuscript. We would also like to thank M.V. Buhler and K. Kamra for their help with the English edition. We thank the corrections and suggestions made from two anonymous reviewers of Journal of South American Earth Sciences journal, that improved this work. We highly appreciate the support of the Municipality of Plaza Huincul and the Municipality of Las Lajas. Institutional support from CONICET and the Universidad Nacional de Río Negro is also greatly acknowledged.

Funding: This work was supported by PIP-CONICET grants # 0233, # 0683, UNRN-PI 40-A-157, 297, 378 grants (to R.A. Coria), UNRN-PI 40-A-698 grants (to M.A. Tunik), PUE 0031CO grants (to S. Casadío) and Municipalidad de Las Lajas (Neuquén). PhD Project registered at Universidad Nacional de Río Negro (by D. Pino).

References

Aguirre-Urreta, B., Schmitz, M., Lescano, M., Tunik, M., Rawson, P.F., Concheyro, A., Buhler, M., Ramos, V.A., 2017. A high precision U–Pb radioisotopic age for the Agrio Formation, Neuquén basin, Argentina: implications for the chronology of the hauterivian stage. Cretac. Res. 75, 193–204. https://doi.org/10.1016/j.cretres.2017.03.027.

Aguirre-Urreta, B., Rawson, P., Concheyro, G., Bown, P., Ottone, E., 2005. Lower cretaceous (Berriasian–Aptian) biostratigraphy of the Neuquén basin. Neuquén basin, Argentina A case study seq. Stratigr. Basin Dyn. https://doi.org/10.1144/GSL.SP.2005.252.01.04.

Alcalá, L., 1994. Macromamíferos neógenos de la fosa de Alfambra-Teruel. Instituto de Estudios Turolenses y Museo Nacional de Ciencias Naurales, p. 554.

Alcala, L., Escorza, C., 1998. Modelling diagenetic bone fractures. Bull. la Société Géologique Fr. 169, 101–108.

Alexander, J., Bridge, J., Cheel, R., Leclair, S., 2001. Bedforms and associated sedimentary structures formed under supercritical water flows over aggrading sand beds. Sedimentology 48, 133–152. https://doi.org/10.1046/j.1365-3091.2001.00357.x.

Araújo-Júnior, H., Bissaro-Júnior, M., 2017. Tafonomia de vertebrados em ambientes continentais. In: Horodyski, R.S., Fernando, E., Org (Eds.), Tafonomia: Métodos, Processos e Aplicação. Editora CRV, pp. 175–236.

Behrensmeyer, A., 1991. Terrestrial vertebrate accumulations. In: Allison, P.A., Briggs, D.E.G. (Eds.), Taphonomy: Releasingthe Data Locked in the Fossil Record, 291–335. Plenum Press, New York.

Behrensmeyer, A., 1975. The taphonomy and paleoecology of Plio-Pleistocene vertebrate assemblages east of Lake Rudolf, Kenya. Bulletin of the Museum of Comparative Biology, Harvard 146, 473–578.

Bonaparte, J.F., 1991. The Gondwanian theropod families Abelisauridae and Noasauridae. Hist. Biol. 5, 1–25. https://doi.org/10.1080/10292389109380385.

Calvo, J., Gonzalez Riga, B., 2003. Rinconsaurus caudamirus gen. et sp. nov., a new titanosaurid (Dinosauria, Sauropoda) from the Late Cretaceous of Patagonia, Argentina. Rev. Geol. Chile 30. https://doi.org/10.4067/S0716-02082003000200011.

Calvo, J., Porfiri, J., Veralli, Novas, F., Poblete, 2004. Phylogenetic status of Megaraptor namunhuaiquii Novas based on a new specimen from Neuquén, Patagonia, Argentina. Ameghiniana 4, 565–575.

Casal, G., Martínez, R., Ibiricu, L., González Riga, B., Foix, N., 2013. Tafonomía del dinosaurios terópodo Aniksosaurus darwini, Formación Bajo Barreal, Cretácico Tardío de la Patagonia (Argentina). Ameghiniana 50, 571–592.

Coria, R., Ortega, F., Succar, C., Currie, P., Koppelhus, E., 2012. First Record of a Dicraeosaurid Sauropod from the Lower Cretaceous (Valanginian) of Neuquén Basin.

Coria, R., Currie, P., Koppelhus, E., Braun, A., Cerda, I., 2010. First record of a valanginian (early cretaceous) dinosaur association from south America. 70th Annual Meeting of the Society of Vertebrate Paleontology. Society of Vertebrate Paleontology.

Coria, R., Currie, P., Currie, C., 2006. A new carcharodontosaurid (dinosauria, theropoda) from the upper cretaceous of Argentina. Geodiversitas 28, 71–118.

Coria, R., Currie, P., Ortega, F., Baiano, M., 2020. An early cretaceous, medium-sized carcharodontosaurid theropod (dinosauria, saurischia) from the Mulichinco Formation (upper valanginian), Neuquén province, patagonia, Argentina. Cretac. Res. https://doi.org/10.1016/j.cretres.2019.104319, 104319.

Coria, R., Ortega, F., Currie, P., Previtera, E., Cardenas, M., 2013. An early cretaceous dinosaur assemblage from the neuquen basin, patagonia, Argentina. XXVII Jornadas Argentinas Paleontología de Vertebrados. 50, 31.

Coria, R., Salgado, L., 1995. A new giant carnivorous dinosaur from the Cretaceous of Patagonia. Nature. https://doi.org/10.1038/377224a0.

Coria, R., Windholz, G., Ortega, F., Currie, P., 2019. A new dicraeosaurid sauropod from the lower cretaceous (Mulichinco Formation, valanginian, Neuquén basin) of Argentina. Cretac. Res. 93, 33–48. https://doi.org/10.1016/j.cretres.2018.08.019.

D'Elia, L., Bilmes, A., Naipauer, M., Vergani, G., Muravchik, M., Franzese, J., 2020. The syn-rift of the Neuquén basin (precuyano and lower cuyano cycle): review of structure, volcanism, tectono-stratigraphy and depositional scenarios. In: Kietzmann, D., Folguera, A. (Eds.), Opening and Closure of the Neuquén Basin in the Southern Andes, pp. 3–21.

Fernández Jalvo, Y., Andrews, P., 2003. Experimental effects of water abrasion on bone fragments. Journal of Taphonomy 1, 147–163.

Fiorillo, A., 1988. Taphonomy of hazard homestead quarry (ogallala group), hitchcock county, Nebraska. In: Contributions to Geology, vol. 26. University of Wyoming, Laramie, pp. 57–97.

Gnaedinger, S., Coria, R., Koppelhus, E., Casadío, S., Tunik, M., Currie, P., 2017. First lower cretaceous record of podocarpaceae wood associated with dinosaur remains from patagonia, Neuquén province, Argentina. Cretac. Res. 78, 228–239. https://doi.org/10.1016/j.cretres.2017.06.014.

Gulisano, C., Gutiérrez Pleimling, A., Digregorio, R., 1984. Esquema estratigráfico de la secuencia jurásica del oeste de la provincia del Neuquén.

Hill, A., 1979. Disarticulation and scattering of mammal skeletons. Paleobiology. https://doi.org/10.1017/s0094837300006552.

Hill, A., Behrensmeyer, A., 1984. Disarticulation Patterns of Some Modern East African Mammals. Paleobiology 10, 366–376. https://doi.org/10.1017/S0094837300008332.

Kietzmann, D., Folguera, A., 2020. Opening and Closure of the Neuquén Basin in the Southern Andes, Springer Earth System Sciences. Springer International Publishing.

Leanza, H., 2009. Las principales discordancias del Mesozoico de la Cuenca Neuquina según observaciones de superficie. Revista del Museo Argentino Ciencias Naturales. Nueva Serie 11, 145–184. https://doi.org/10.22179/REVMACN.11.257.

Leanza, H., Apesteguía, S., Novas, F., de la Fuente, M., 2004. Cretaceous terrestrial beds from the Neuquén Basin (Argentina) and their tetrapod assemblages. Cretac. Res. 25, 61–87. https://doi.org/10.1016/j.cretres.2003.10.005.

Lyman, R., 1994. Vertebrate Taphonomy. Cambridge University Press, Cambridge.

Martinez, L., Olivo, M., Koppelhus, E., Coria, R., 2012. First Record of Tempskya Corda from Mulichinco Formation (Valanginian), Sierra De La Vaca Muerta. Neuquén Basin, Argentina.

Martin, R.E., 1999. Taphonomy: A process approach. Cambridge University Press, Cambridge.

Martínez, L., Olivo, M., 2015. Tempskya in the valanginian of South America (Mulichinco Formation, Neuquén basin, Argentina) - systematics, palaeoclimatology and palaeoecology. Rev. Palaeobot. Palynol. 219, 116–131. https://doi.org/10.1016/j.revpalbo.2015.04.002.

McCabe, P., Jones, C., 1977. Formation of reactivation surfaces within superimposed deltas and bedforms. J. Sediment. Res. 47, 707–715. https://doi.org/10.1306/212F722A-2B24-11D7-8648000102C1865D.

Miall, A., 2014. Fluvial Depositional Systems, Fluvial Depositional Systems. Springer International Publishing. https://doi.org/10.1007/978-3-319-00666-6.

Miall, A., 1996. The Geology of Fluvial Deposits: Sedimentary Facies, Basin Analysis, and Petroleum Geology. https://doi.org/10.1016/s0037-0738(96)00081-4.

Miall, A., 1978. Lithofacies types and vertical profile models in braided river deposits: a summary. Fluv. Sedimentol. 5, 597–600.

Mpodozis, C., Ramos, V., 2008. Tectónica Jurásica en Argentina y Chile: extensión, subducción oblicua, rifting, deriva y colisiones? Rev. Asoc. Geol. Argent. 63, 481–497.

Nanson, G., Croke, J., 1992. A genetic classification of floodplains. Geomorphology. https://doi.org/10.1016/0169-555X(92)90039-Q.

Nemec, W., Postma, G., 1993. Quaternary Alluvial Fans in Southwestern Crete: Sedimentation Processes and Geomorphic Evolution, pp. 235–276. https://doi.org/10.13140/2.1.1535.5521.

Norman, D.B., 1987. A Mass-accumulation of vertebrates from the Lower Cretaceous of Nehden (Sauerland), West Germany. In: Proceedings of the Royal Society of London. Series B: Biological Sciences, pp. 215–255.

Noto, C.R., 2011. Hierarchical Control of Terrestrial Vertebrate Taphonomy Over Space and Time: Discussion of Mechanisms and Implications for Vertebrate Paleobiology BT - Taphonomy: Process and Bias Through Time. Springer, Netherlands, Dordrecht, pp. 287–336. https://doi.org/10.1007/978-90-481-8643-3_8.

Novas, F., 1996. Alvarezsauridae, cretaceous basal birds from patagonia and Mongolia. Memoirs of Queensland Museum.

Paulina Carabajal, A., Coria, R., Currie, P., Koppelhus, E., 2018. A natural cranial endocast with possible dicraeosaurid (Sauropoda, Diplodocoidea) affinities from the Lower Cretaceous of Patagonia. Cretac. Res. 84, 437–441. https://doi.org/10.1016/j.cretres.2017.12.001.

Previtera, E., 2019. Taphonomic analysis of saurischian dinosaurs from the plottier formation (Upper cretaceous), Mendoza, Argentina. Andean Geol. 46, 345–367. https://doi.org/10.5027/andgeov46n2-3161.

Previtera, E., 2017. Microestructura ósea y diagénesis de dinosaurios saurisquios del Cretácico Superior (Grupo Neuquén), Argentina. Andean Geol. 44, 39–58. https://doi.org/10.5027/andgeoV44n1-a03.

Previtera, E., 2011. Tafonomía de dinosaurios de la cuenca Neuquina sur mendocina. Tesis Doctoral.

Ramos, V., Folguera, A., 2009. Andean flat-slab subduction through time. Geol. Soc. London, Spec. Publ. 327, 31–54. https://doi.org/10.1144/SP327.3.

Quattrocchio, M., Martínez, M., García, V., Zavala, C., 2003. Palinoestratigrafía del Tithoniano-Hauteriviano del centro-oeste de la Cuenca Neuquina, Argentina. Revista Española de Micropaleontología 35, 51–74.

Ramos, V., 1999. Plate tectonic setting of the andean cordillera. Episodes 22, 183–190. https://doi.org/10.18814/epiiugs/1999/v22i3/005.

Reesink, A., Bridge, J., 2011. Evidence of bedform superimposition and flow unsteadiness in unit-bar deposits, south saskatchewan river, Canada. J. Sediment. Res. 81, 814–840. https://doi.org/10.2110/jsr.2011.69.

Rossel, P., Carvajal, F., 2020. Early andean magmatism in southern Central Chile (33°–40° S). Opening and Closure of the Neuquén Basin in the Southern Andes, pp. 107–126.

Salgado, L., Coria, R., Calvo, J., 1997. Evolution of titanosaurid sauropods. I: phylogenetic analysis based on the postcranial evidence. Ameghiniana 34, 3–32.

Schwarz, E., 2003. Análisis paleoambiental y estratigrafía secuencial de la Formación Mulichinco en el sector septentrional de la provincia del Neuquén, Cuenca Neuquina, Argentina. Tesis Doctoral. Universidad Nacional de La Plata.

Schwarz, E., Spalletti, L., Howell, J., 2006. Sedimentary response to a tectonically induced sea-level fall in a shallow back-arc basin: the Mulichinco Formation (Lower Cretaceous), Neuquén Basin, Argentina. Sedimentology 53, 55–81. https://doi.org/10.1111/j.1365-3091.2005.00753.x.

Shipman, P., Bosler, W., Davis, K.L., 1981. Butchering of giant Geladas in an Acheulian site. Curr. Anthropol. 22, 257–268. https://doi.org/10.1086/202663.

Smith, S., Edwards, R., 1991. Regional sedimentological variations in lower triassic fluvial conglomerates (budleigh salterton pebble beds), southwest england: some implications for palaeogeography and basin evolution. Geol. J. 26, 65–83. https://doi.org/10.1002/gj.3350260105.

Stipanicic, P., Rodrigo, F., Baulies, O., Martínez, C., 1968. Las formaciones presenonianas en el denominado Macizo Nordpatagónico y regiones adyacentes. Rev. Asoc. Geol. Argent. 2, 367–388.

Todd, L., Frison, G., 1986. Taphonomic study of the colby site mammoth bones. In: Frison, G.C., Todd, L.C. (Eds.), The Colby Mammoth Site. University of New Mexico Press, Albuquerque, pp. 27–90.

Todd, L., 1983. Taphonomy: Fleshing Out the Dry Bones of Plains Prehistory.

Voorhies, M., 1969. Taphonomy and population dynamics of an early pliocene vertebrate fauna, knox county, Nebraska. Taphon. Popul. Dyn. An Early Pliocene Vertebr. Fauna, Knox County, Nebraska. https://doi.org/10.2113/gsrocky.8.special_paper_1.1.

Weaver, C., 1931. Paleontology of the Jurassic and Cretaceous of West Central Argentina. University of Washington press.

Wood, J.M., Thomas, R.G., Visser, J., 1988. Fluvial processes and vertebrate taphonomy: The Upper Cretaceous Judith River Formation, south-central Dinosaur Provincial Park, Alberta, Canada. Palaeogeogr. Palaeoclimatol. Palaeoecol. 66, 127–143.

Schwarz, E., Spalletti, L.A., Veiga, G.D., 2011. La Formación Mulichinco (Valanginiano). In: Leanza, H., Arregui, C., Carbone, O., Danieli, J.C., Vallés, J. (Eds.), Geología y Recursos Naturales de la provincia del Neuquén, pp. 131–144. Congreso Geológico Argentino, No. 18, Actas.